UNIVERSITY OF OKLAHOMA

GRADUATE COLLEGE

EXPERIMENTAL AND NUMERICAL STUDY ON SEPARATION OF SOLID-LIQUID SLURRIES

A THESIS

SUBMITTED TO THE GRADUATE FACULTY

in partial fulfillment of the requirements for the

Degree of

MASTER OF SCIENCE

By

HOOTAN RAHIMI
NORMAN, OKLAHOMA
2020

EXPERIMENTAL AND NUMERICAL STUDY ON SEPARATION OF SOLID-LIQUID SLURRIES

A THESIS APPROVED FOR THE
SCHOOL OF AEROSPACE AND MECHANICAL ENGINEERING

BY THE COMMITTEE CONSISTING OF

Dr. Hamidreza Shabgard, Chair

Dr. Ramkumar Parthasarathy

Dr. Jie Cai

To my wife and parents
for their love and support

Abstract

The separation of solid-liquid slurries, as a critical stage of a novel zero-liquid discharge (ZDL) eutectic-freeze desalination method, is the focus of this thesis. Firstly, various technologies for separation of solid-liquid slurries are examined and the most suitable methods are identified, namely, hydrocyclone separator and hydraulic wash column. Experimental and numerical studies were performed for each separation method and results and discussions were provided. The experimental study of the cyclone separator using various water-based slurries showed that pure water could be recovered from the slurry when the solid particles had a sufficiently greater density than the water. For solid particles lighter than water, however, pure water could not be recovered and both outlet streams contained different amounts of solid particles. The numerical results from the hydraulic wash column model predicted an optimum inlet flow velocity for the column and the experiments were performed successfully for a batchwise separation process. Recommendations were made for enabling continuous separation process using the wash column.

Keywords: Separation, solid-liquid slurry, hydrocyclone, hydraulic wash column.

Table of Contents

1. Introduction 1

1.1. Solid-liquid separation methods 2

1.2. Thesis organization 3

2. Experimental and Numerical Study on Hydrocyclone Separator 4

2.1. Background and literature review 4

2.2. Numerical study on hydrocyclone separator 7

2.3. Experimental study on hydrocyclone separator 14

2.3.1. Experimental setup 14

2.3.2. Results and discussions 17

3. Numerical and Experimental Study on Hydraulic Wash Column 25

3.1. Background and literature review 25

3.2. Numerical study on hydraulic wash column 29

3.3. Experimental study on hydraulic wash column 40

4. Conclusions 50

References 51

1. Introduction

Solid-liquid separation processes are found in a wide range of industrial applications. Several approaches have been employed to separate various components from solid-liquid slurries. The separation of solid-liquid slurries as the final stage of a novel zero-liquid discharge (ZDL) eutectic-freeze desalination method, is the focus of this thesis. The solid-liquid slurry includes brine, intermediate cold liquid (ICL) and the ice particles. The pure ice crystals are formed within a highly concentrated brine by direct injection of an intermediate cold liquid (ICL). The production of 9 barrels of brine from every barrel of extracted oil is the main motivation of the research and proposed ZDL model. Disposing of such produced water poses a serious challenge to the environment. In addition, it is of great importance to introduce methods which mitigates the environmental concerns and is economical in the competition for freshwater production.

The proposed method has many unique features such as superior heat transfer rate compared to indirect freeze desalination methods, less energy requirement than evaporative methods and not utilizing any types of chemicals or contaminants in the process. Also, the ZDL desalination unit will be able to handle high dissolved solid concentration, for example, input total dissolved solid (TDS) up to 300,000 ppm and output TDS of less than 1000 ppm. In addition, the system operates at atmospheric pressure.

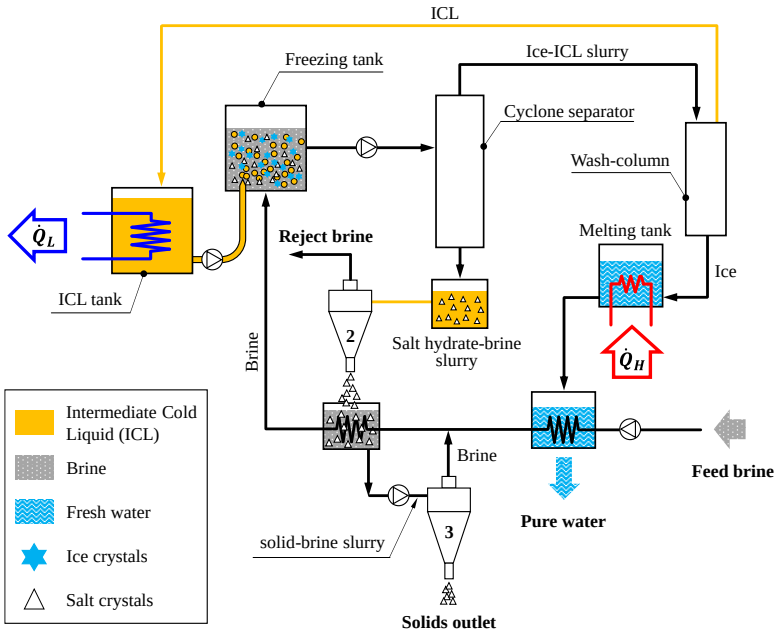

Figure 1. Material flow diagram of the innovative freeze-desalination system

1.1. Solid-liquid separation methods

Attempts have been made to categorize the variety of processes and machines used in solid-liquid separation systems; these are usually based on two principal modes of separation [1]:

1. Filtration, in which the solid-liquid mixture is directed towards a “medium” (screen, paper, woven cloth, membrane, etc.). The liquid phase or filtrate flows through the latter whilst solids are retained, either on the surface, or within the medium.

2. Separation by Sedimentation or Settling in a force field (gravitational, centrifugal) Wherein advantage is taken of differences in phase densities between the solid and the liquid. The solid is allowed to sink in the fluid, under controlled conditions. In the reverse process of flotation, the particles rise through the liquid by virtue of a natural or induced low “solids” density.

The filterability and sedimentation velocity of solid-liquid mixtures depend on the state of dispersion of the suspension; in turn, the latter is strongly influenced by solid-liquid surface conditions which govern the stability of the mixture and the overall result of particle-particle contact. The dispersive and agglomerative forces present in these systems are functions of temperature, agitation, pumping conditions, etc. all of which complicate the situation and produce the result that suspension properties cannot be explained m hydrodynamic terms alone.

A first step in the design of a separation system is to choose the most appropriate technology from filtration, sedimentation, or a combination of these two methods. In general, sedimentation techniques are cheaper than those involving filtration; the use of gravity settling would be considered first, particularly where large, continuous liquid flows are involved. A small density difference between the solid and fluid phases would probably eliminate sedimentation as a possibility, unless the density difference can be enhanced, or the force field of gravity increased by centrifugal action. Such techniques for enhancing sedimentation would be retained as a possibility in those circumstances where gravity separation proves to be impossible, and the nature of the particulates was such as to make filtration “difficult”. The latter condition would ensue when dealing with small, sub-micron material, or soft, compressible solids of the type encountered in wastewater and other effluents. Some separations require combination of the processes of sedimentation and filtration;

preconcentration of the solids will reduce the quantity of liquid to be filtered and, therefore, the size of filter needed for the separation.

Another serious consideration is whether the separation process is conducted continuously or discontinuously; the latter method is known as ‘batch” processing. In this case, the separator acts intermittently between filling and discharge stages. The concentration of solids in the feed mixture and the quantities to be separated per unit time are also factors which affect the selection procedure. It will be apparent that in the development of a typical process for: (a) increasing the solids concentration of a dilute feed, (b) pretreatment to enhance separation characteristics, (c) solids separation, (d) de-liquoring and washing, many combinations of machine and technique are possible. Some of these combinations may result in an adequate, if not optimal, solution to the problem. Full optimization would inevitably be time consuming and expensive, if not impossible in an industrial situation [1].

1.2. Thesis organization

The separation stage is the last step to produce desalinate water in the ZDL desalination unit. It is extremely important to extract the ice particles from the final brine-ice-ICL slurry with the highest possible purity, so the final product of the system meets the contaminant criteria standards. Numerical and experimental studies were conducted to investigate the best way to perform the separation. Computational fluid dynamic study of both hydrocyclone and hydraulic wash column was conducted to gain fundamental understanding of multiphase and multiscale transport phenomena occurring within the separation stage. Furthermore, laboratory prototypes of both hydrocyclone separator and wash column has been fabricated and lab-scale experiments on separation within a slurry system comprised of brine and ICL has been designed and tested.

The current thesis explores the numerical and experimental studies on both hydrocyclone separator and hydraulic wash column and provides the results from the conducted tests. Finally, the pros and cons of each technique was described and the most satisfying method to separate the ice crystals from the slurry and produce pure water was introduced.

2. Experimental and Numerical Study on Hydrocyclone Separator

A comprehensive numerical and experimental study is performed on the behavior of hydrocyclone separator. A brief background and literature review is presented to better understand the principles of hydrocyclones and previous studies in the literature. The numerical model and its results is explained in details followed by the experimental setup information and results. It was shown by the experimental results that the utilized hydrocyclone performs a complete separation while using solid particles with higher density than the liquid phase, however, it was not able to provide complete separation while utilizing solid particles with lower than liquid phase density.

2.1. Background and literature review

Centrifugal separation makes use of an enhanced field force over that provided by gravity to cause particle or liquid motion and can be used for liquid-liquid separation as well as liquid-solid separation. Centrifuges may be divided into two main categories: firstly, those that separate using a sedimentation principle and employing a solid, or imperforated bowl; and secondly those that use a filtration principle employing a perforated bowl. In the filtering centrifuge, the g-force provides the pressure to force the mother liquor through the cake. Hydrocyclone have much in common with the sedimenting centrifuge, but the energy needed to cause the liquid to rotate comes from the liquid rather than an external mechanical drive [1].

A hydrocyclone is a device employing centrifugal separation without the need for mechanically moving parts, other than a pump. They are cheap, compact, and versatile as a means of solid-liquid separation. It is similar in operation to a centrifuge, but with much larger values of g-force (ranging from 800 g in a 300 mm diameter cyclone to 50000 g in a 10 mm diameter cyclone) [1]. This force is, however, applied over a much shorter residence time. The most significant difference in the fluid mechanics between the centrifuge and the hydrocyclone is that the liquid in the former rotates as a solid body with constant angular velocity, a forced vortex, whereas the hydrocyclone approaches constant angular momentum conditions, a free vortex. A density difference between the dispersed phase and liquid is an essential requirement for both hydrocyclone and centrifuge. As this density difference reduces so does the effectiveness of the centrifugal separator. The residence time inside a centrifuge could be extended to compensate for a low-density difference and even batch centrifugation is possible.

A similar option does not exist with hydrocyclone. Subject to a significant density difference, hydrocyclone can be effective in separating particles down to 2 μm in diameter, below this size the efficiency is lowered by the complex flow patterns and turbulence inside the cyclone.

The most noticeable flows in the hydrocyclone are the primary and secondary vortices. The primary vortex lies outside the secondary one and carries suspended material down the axis of the hydrocyclone.

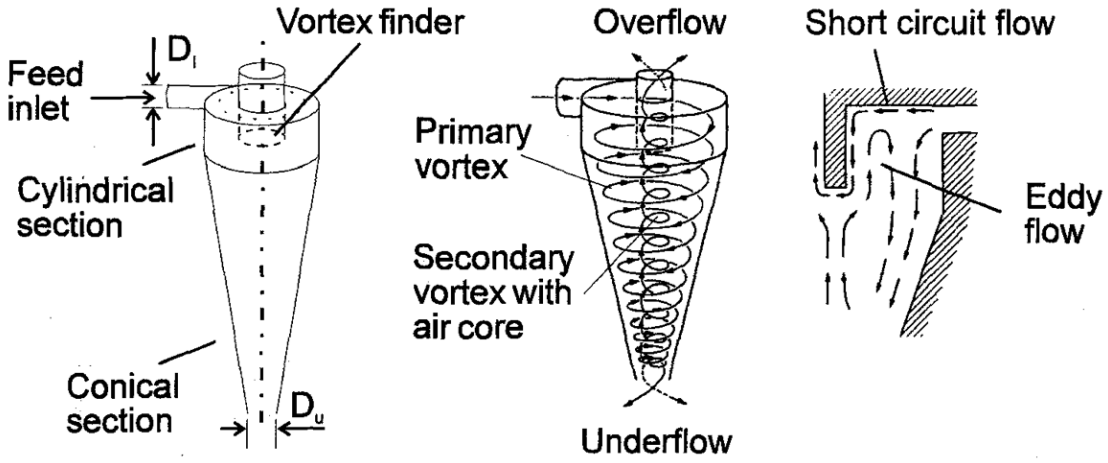

Figure 2 Principle features and flows inside a hydrocyclone [1]

The secondary vortex carries material up the axis and into the overflow vortex finder. There is also an air core of a few millimeters' diameter at the center of the vortices. Some of the suspended material "short-circuits" the vortices by leaking around the top of the hydrocyclone and into the overflow. The vortex finder design is important in reducing this loss of unclassified material. Hydrocyclone can act as classifiers and/or thickeners; the overflow being a dilute suspension of fine solids, the underflow is a concentrated suspension of more coarse solids [1].

Liquid-solid hydrocyclones are widely used in chemical and petroleum industries due to their advantages, including compact geometry, high separation efficiency and easy maintenance [2]. It has been shown that the liquid-solid separation mainly occurs in the conical part. Increasing the conical height can improve the grade efficiencies[1] for solid particles, especially the smaller

[1] The **grade efficiency** is a way of characterizing how well particles are separated according to size (density, or some other desired property).

ones. Besides, the grade efficiencies would gradually decrease as the cylindrical height increases. Compared to larger solid particles, the grade efficiency for smaller ones is more susceptible to the changes of the cylindrical height.

Wang et al. [2] experimentally proved that the liquid-solid separation depends strongly on the physical properties of the liquid phase, and the grade efficiencies would be improved as the water cut [2] increases, especially for smaller solid particles.

In an experimental study, Dai et al. [3], showed that Not all the solid particles in the inner helical flow discharge with the overflow; some of them also again be moved towards the wall. The particles that move down along the outer wall of the vortex finder lead to the leakage of coarse particles through the overflow, which will affect the separating performance of the hydrocyclone to some extent. They also proved that the size of the solid particles decreases from the wall of the hydrocyclone towards the center. The concentration maximum is not near the hydrocyclone wall, but near the loci of zero velocity lines for the solid particles. Reducing or eliminating the area between the two LZVV lines, which is a low efficiency area, will lead to an increase in the separating efficiency.

Hydrocyclones used for solid–liquid separation are usually composed of a single cone. In a study, Yang et al. [4], designed hydrocyclones with two cone combinations for solid–liquid separation and investigated the flow field and separation performance. Simulation and experimental results showed that when the second cone remained unchanged, the angle change of the first cone had significant effect on the value of three-dimensional velocities, flow split, separation efficiency, energy consumption, and separation sharpness, but little effect on the distribution of pressure and that of three-dimensional velocities, the capacity and cut size. The bigger of the first cone's angle, the smaller of the flow split and the higher the separation efficiency, the stronger of the centrifugal force, and the more the small particles in underflow. The smaller the angle change between the two cones, the larger the sharpness of the grade efficiency curve, i.e., the hydrocyclone is more suitable for the classification process.

Han et al. [5] designed several new types of hydrocyclones for fine particles removal from the liquid by adding internal parts to the underflow section of the typical solid-liquid hydrocyclone.

[2] The ratio of **water** compared to the volume of total mixture.

The results indicated that adding an inner cylinder to the underflow pipe can reduce the Euler number remarkably and has little influence on the separation efficiency. When the conical section length was reduced by about 1/3, the separation efficiency of the hydrocyclone with an inner cylinder decreased only 1.1%~2.0% and was similar to the traditional one under high feed flow rates. Under low feed flow rates, the separation efficiency of this shortened hydrocyclone decreased as high as 5.8%.

In an experimental study, Rocha et al. [6], showed that in hydrocyclones with circular and square feed duct, using a diluted aqueous quartzite suspension (1% v/v), an increases of 7.6% and 12.5% was provided in the underflow-to throughput ratio and Euler number, respectively, and a 32% decrease in the cut size diameter for the square feed duct compared to standard hydrocyclone. Therefore, a simple change in the shape of the hydrocyclone feed duct improves the solids separation performance of equipment previously designed for high separation efficiency.

2.2. Numerical study on hydrocyclone separator

A 3D numerical model of the hydrocyclone was developed in ANSYS Fluent 19.1 to study the behavior and separation performance of the device. Figure 3 shows the geometry and grids of the model. The model is developed with similar dimension as the actual hydrocyclone separator device that was used in the experiments. The geometry has been created in Design Modeler utility in ANSYS Workbench and then imported to the Meshing utility of the Workbench. The final grid was exported as a mesh file into Fluent for numerical analysis. In Fluent, Continuity and momentum equations were solved numerically using a control volume approach.

The surface areas of inlet, overflow and underflow are $1.4e^{-4}$ m^2, $6.35e^{-5}$ m^2 and $1.25e^{-5}$ m^2, respectively. The numerical model included 907168 elements and was separated into 8 different zones for enhanced the mesh quality.

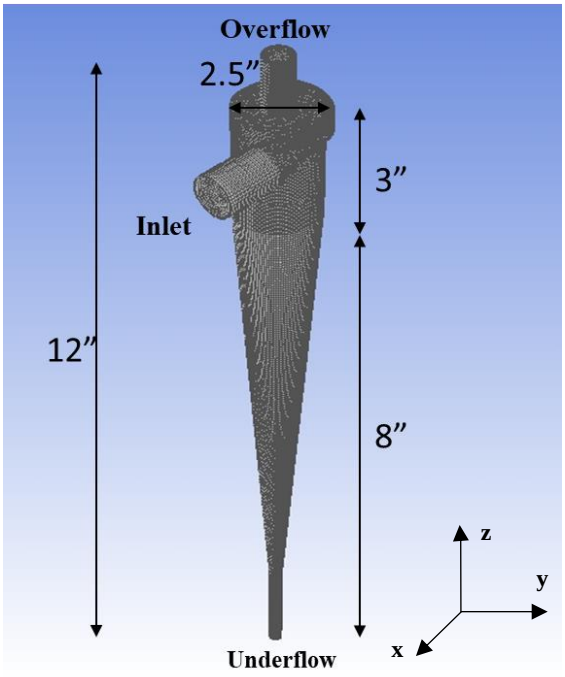

Figure 3 Geometry and grid mesh of the hydrocyclone CFD model

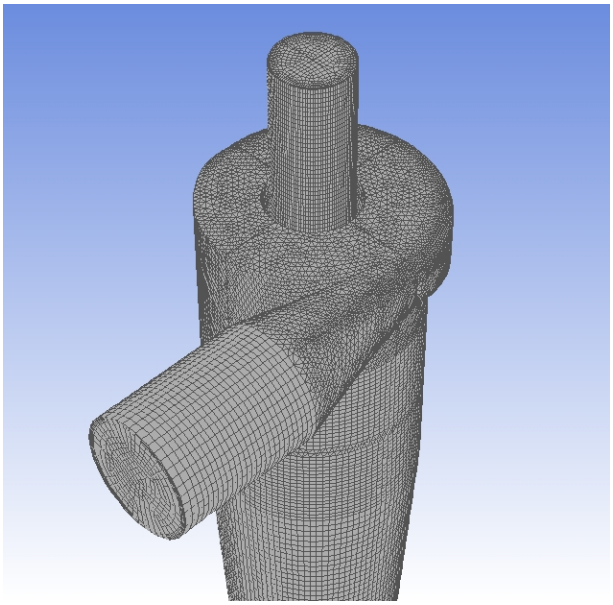

Figure 4. Close up view of the upper half of the CFD model, variety of zones and mesh qualities

A steady state pressure-based solver was equipped to study the separation of both salt and ice particles with 1650 kg/m^3 and 920 kg/m^3 densities. The fluid in the model was chosen to be the ICL with 1400 kg/m^3 density. Considering the density of each phase in the numerical model, and the range of flow velocities (from 1 m/s to 10 m/s), the Reynolds number was calculated to have a range from 7490 to 7.49×10^4. This Reynolds number range is clearly

indicating that our flow is turbulent. Therefore, a *k-ε* turbulent viscous model, was chosen along with DPM[3] to track the movement of particles inside the model's domain. The other solver settings related to the *k-ε* are shown in Fig. 5. Salt particles were assumed to have a mean diameter of $5e^{-5}$ m while ice particles were assumed to have a mean diameter of $1.9e^{-5}$ m. Both salt and ice particles were assumed to have a uniform diameter distribution.

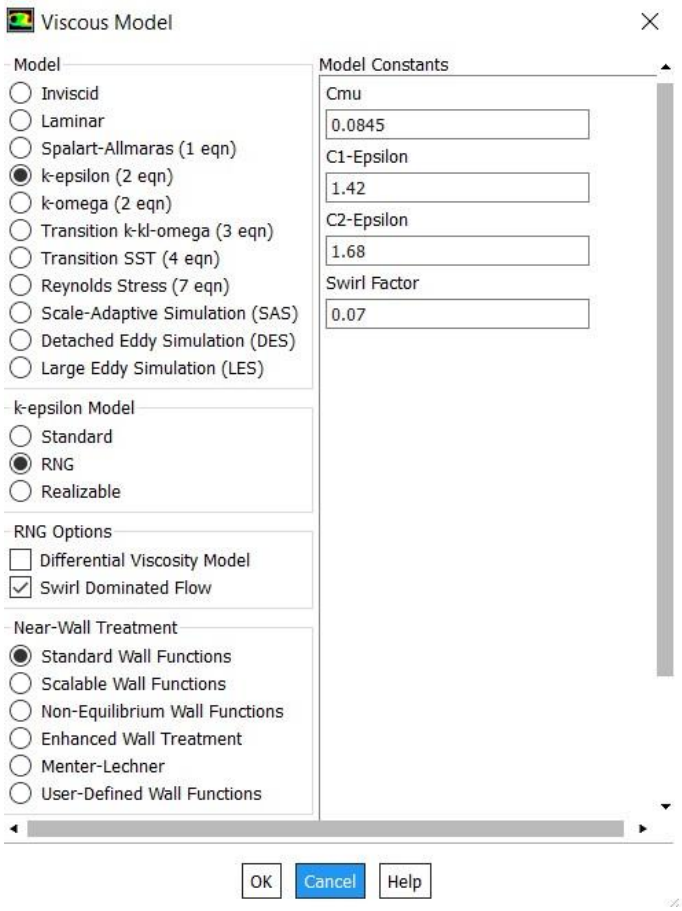

Figure 5. Configuration of the *k-ε* turbulent model in Fluent

Boundary conditions in the model were key factors of the study. Different inlet velocities, from 1 m/s to 10 m/s, and mass flow rates were assigned and tested to investigate the effect of flow rate of the inlet slurry on the separation. Both Overflow and Underflow outlets were assigned a pressure outlet boundary condition with a zero-gauge pressure. The SIMPLE algorithm was used for the pressure velocity coupling, PRESTO! scheme for pressure and Power Law scheme for both momentum and turbulent dissipation rate.

[3] Discrete Phase Model

The separation performance and efficiency of the hydrocyclone model were first studied using single solid phase slurry. For this purpose, salt-ICL and ice-ICL slurries were modeled with properties described before. The results from each case are discussed in the following.

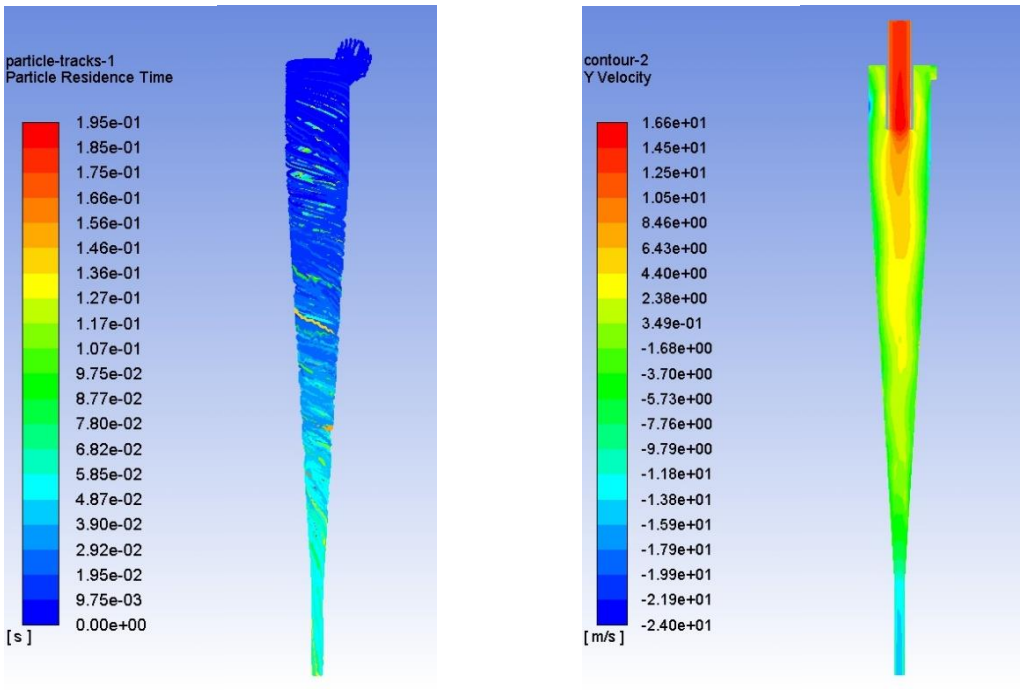

(a) (b)

Figure 6. CFD results of the salt-ICL slurry separation in the hydrocyclone, (a) particle residence time (b) velocity contour

Figure 6 shows the salt particles residence time in the model and also the velocity in the *y* direction on the *x-y* plane. Among 1010 particles which were tracked in every injection, all completed the track and there was no incomplete tracked particle. The particle residence time shown in Fig. 6a indicates that the salt particles tend to move towards the underflow as the time goes by. This is in ordinance with the expectations regarding the hydrocyclones. The heavier phase always tends to move towards the bottom outlet in the device as it faces the centrifugal force created by the flow into the cyclone. Also, considering the time frame in which the salt particles form a smooth path line to the underflow discharge, our numerical results indicate that this happens very fast, meaning that the separation via centrifugal force in the hydrocyclone is proven by our model. In addition, the expected fact that zero salt particle got discharged from the overflow, validates our model in which separation occurs based on density difference and heavier phase has been discharged from the expected underflow. The Y velocity contour in Fig. 6b, shows the elevation of flow velocity after entering into the hydrocyclone.

The *y* velocity in both overflow and underflow has been elevated almost 3 times the initial inlet velocity of 6.41 m/s in this case.

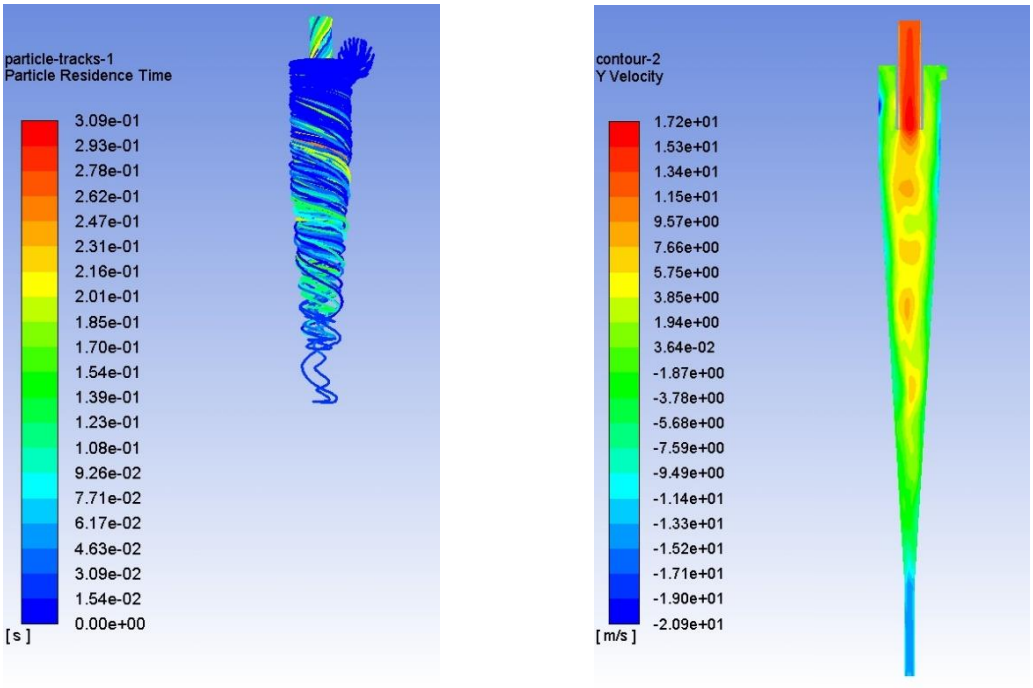

(a) (b)

Figure 7. CFD results of the ice-ICL slurry separation in the hydrocyclone, (a) particle residence time (b) velocity contour

The ice particles residence time and velocity contour in the *y* direction on the *x*-*y* plane of the case with ice-ICL slurry is shown in Fig. 7. The particle residence time graph, Fig. 7a, indicates that ice particles tend to move towards the overflow discharge as time goes on. Considering the densities of each phase in the model, ice particles with 920 and ICL with 1400 Kg/m^3, it was expected to get the separated ice particles discharged from the overflow. The numerical results proved that the model is in comply with the expected separation of solid liquid phases in the hydrocyclone. Also, as it was seen in the previous section, no ice particle got discharged from the underflow outlet which validates the model in the sense that the lighter phase gets discharge only from the top outlet. Figure 7b shows the *y*-direction velocity in the hydrocyclone domain. Similar to the case with the salt and ICL, the flow velocity elevates after entering the hydrocyclone and more specifically the highest velocity occurs right inside the vortex finder and underflow outlet right after where the separation is happening.

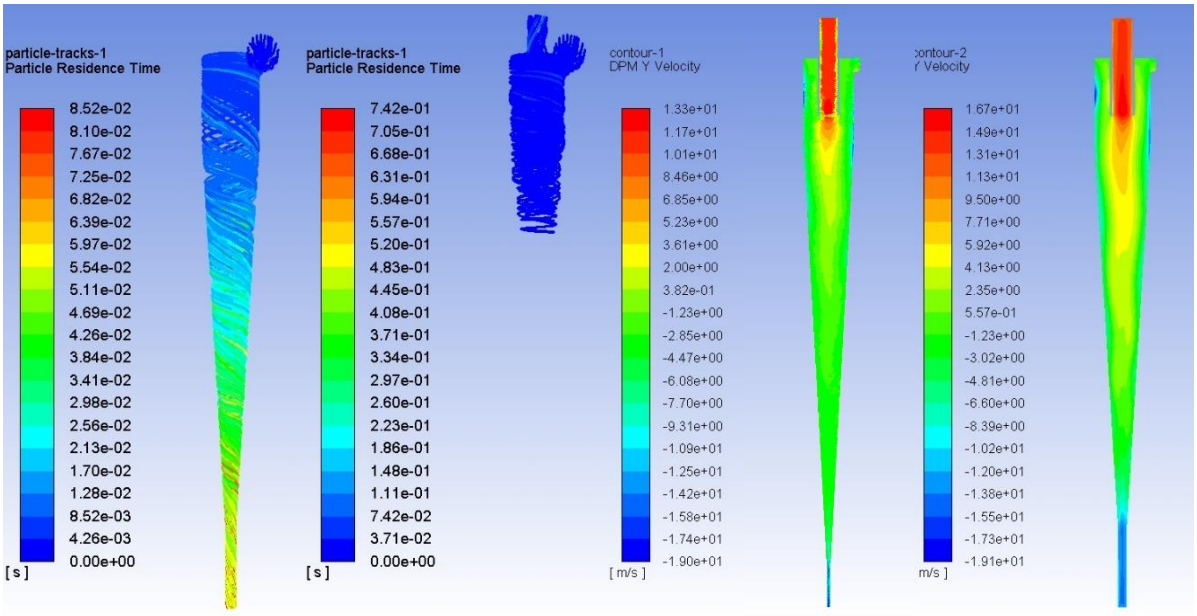

(a) (b) (c) (d)

Figure 8. CFD results for separation of the ice-ICL-salt slurry in the hydrocyclone model, (a) Particle residence time (salt particles) (b) Particle residence time (ice particles) (c) DPM Y velocity contour (d) y-velocity contour

After studying the separation behavior of the hydrocyclone using only one solid phase inside the slurry, a case with both salt and ice particles was conducted inside the mixture that runs through the device. Figure 8a and 8b shows the particle residence time for each solid phase separately. As it was proved in the previous section, salt particles tend to discharge from the underflow and ice particles tend to discharge from the overflow considering the densities of each phase. The interesting observation comes from the Fig. 8c in which the DPM Y velocity contour is shown. It is of great importance to notice that after particles get separated in hydrocyclone and moving toward their desired discharge outlet, they tend to move near the walls with higher velocities. The refined boundary layer mesh in the domain has helped to point this phenomenon out. In Fig. 8d, the Y-direction velocity contour is shown. Comparing this contour with Fig. 8c, reveals that particles tend to move slower than the liquid phase (ICL) in the domain. As it is shown in these contours, the velocity of the fluid phase elevates more than 3 times the velocity of the particles.

To validate our CFD[4] model, a similar experimental work was chosen which was done by Monredon et al. [7], and their work was duplicated in our CFD case. In this study, experimental tests were conducted to validate an analytical model of separation in the hydrocyclones.

[4] Computational Fluid Dynamic

Limestone solid particles with a variety of particle diameters were chosen as the solid phase and water was chosen as the liquid phase. Five different hydrocyclone dimension sets are introduced in this study which were categorized into 2 different groups based on the cone angle (15^o & 20^o) and height. The duplicated CFD case included and studied both latter groups. Figure 9 shows the geometry of each hydrocyclone group and also the generated mesh.

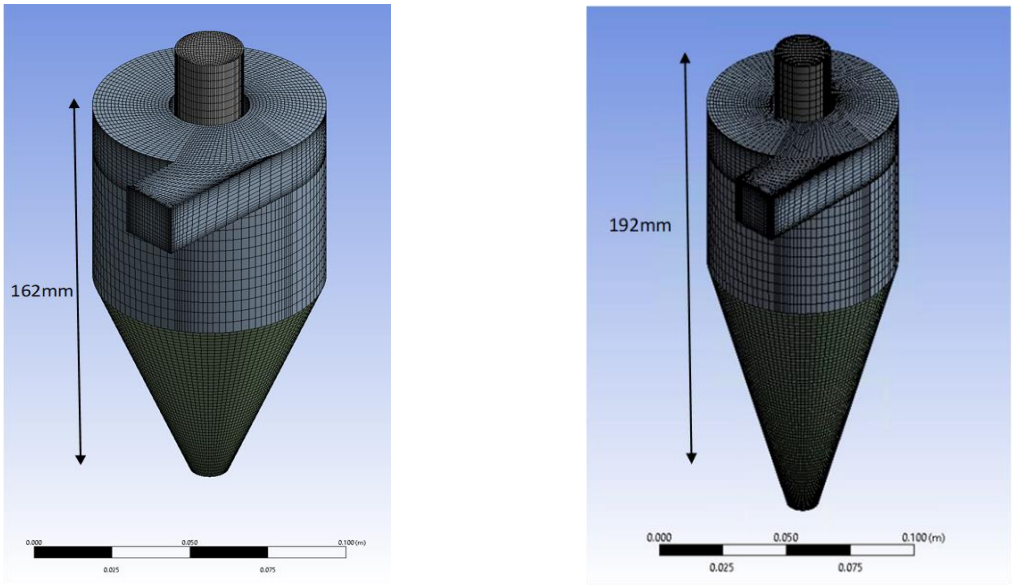

(a) (b)

Figure 9. Generated Geometry and Mesh from the Monredon [7], (a) spigot angle 20°, (b) spigot angle 15°

The operating conditions of the Monredon study were imitated in our CFD study to get the results of the separation and comparing them with actual experiment results. In the Monredon experiment a wide range of slurry flow rates have been tested from around 5 to 50 GPM. Also, they have utilized Limestone solid particles with 2160 kg/m^3 and different slurry mixtures of 5, 10 and 20 weight percentages with water. Results from our numerical analysis agrees satisfactorily with the experiment results which validates our model. As it is shown in Fig. 10, for the case of a 15^o spigot and 192 mm height, the separation ratio increases by the increase in the flow rate and while for lower flow rates the agreement between experimental and numerical results are proven, as the flow rates increases, there is a growing discrepancy between the separation ratios but still close enough for agreement to stand.

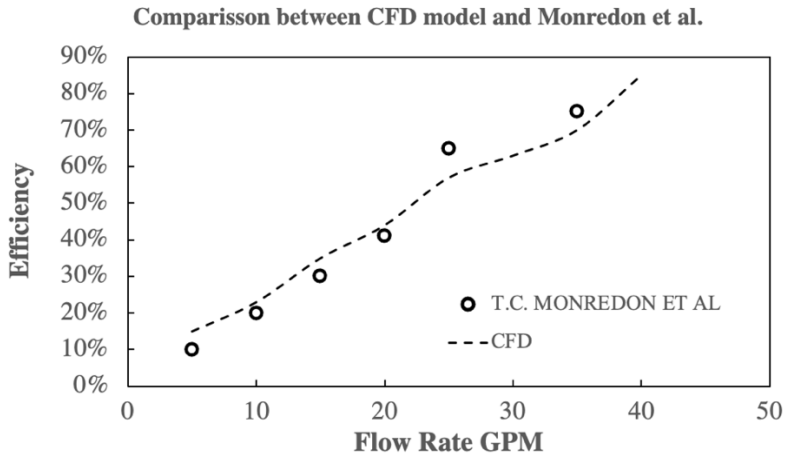

Figure 10. Comparison between experimental results [7] and numerical analysis

The experimental study of the hydrocyclone separation is reviewed in the next section. In this study, the effort was to simulate the actual Ice-Brine-ICL separation using a lab scale hydrocyclone setup.

2.3. Experimental study on hydrocyclone separator

2.3.1. Experimental setup

A laboratory scale separation setup was designed and built to run experiments using a hydrocyclone. The setup was consisting of a pump, flow meter, pressure transducer and hydrocyclone. Figure 11 shows the schematic of the set up.

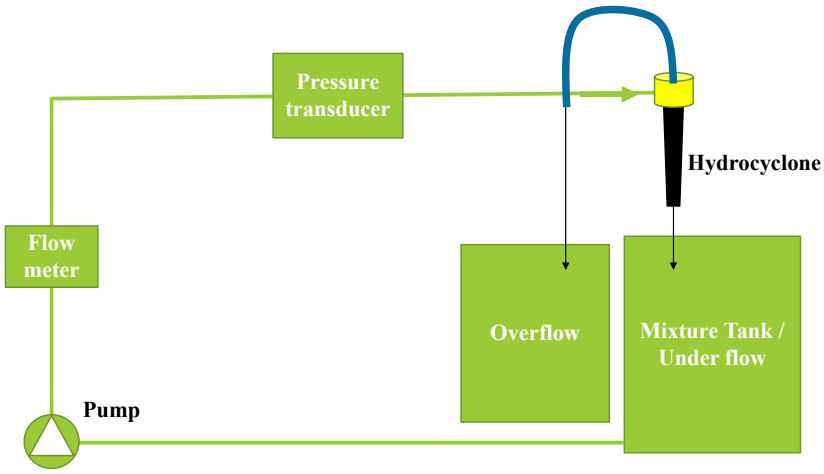

Figure 11. Schematic of the hydrocyclone setup

An Iwaki Magnetic drive NRD-20 series pump was utilized in this set up. The pump was capable of producing a maximum flow rate of 6 GPM[5] and a maximum head of 27.9 feet. A Smart Measurement inline electromagnetic flowmeter with a fluid velocity range of 0.01 m/s to 10 m/s is situated in the setup to monitor the flow rate of the running slurries. Also, a Honeywell pressure transducer is located in the setup to monitor the flow pressure just before entering the hydrocyclone. Figure 12 shows the manufactured lab scale setup.

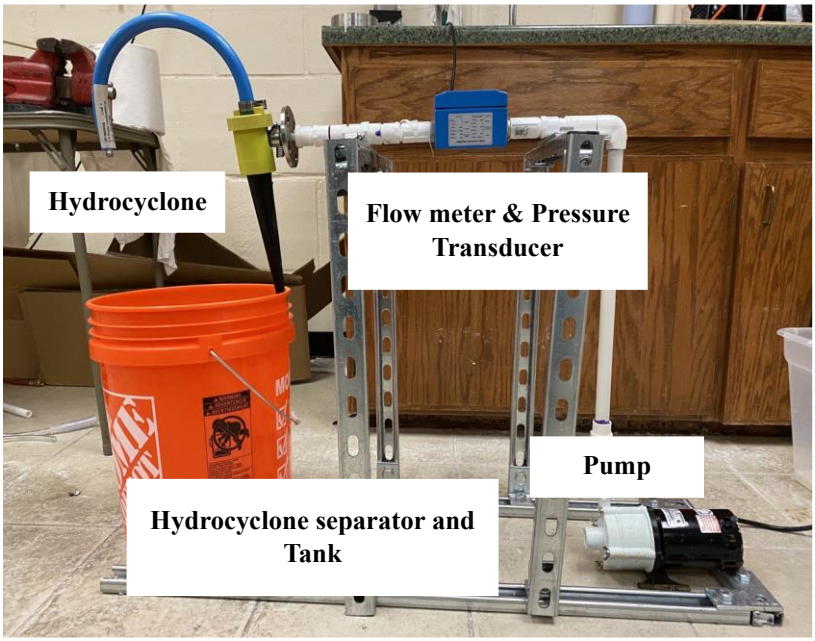

Figure 12. Experimental hydrocyclone setup

A few modifications were made to study the effect of piping size on the separation efficiency of the hydrocyclone setup. To reduce the head loss, the piping was reduced by 1/4 and the hydrocyclone outlets were positioned on the same tank (Fig. 13).

The hydrocyclone model FC25-7 was purchased separately from the Multotec company. The device is consisting of four parts: the inlet, the vortex finder, the underflow (Spigot) and overflow outlets. The schematic of the hydrocyclone is shown in Fig. 14.

[5] US Gallons per Minute.

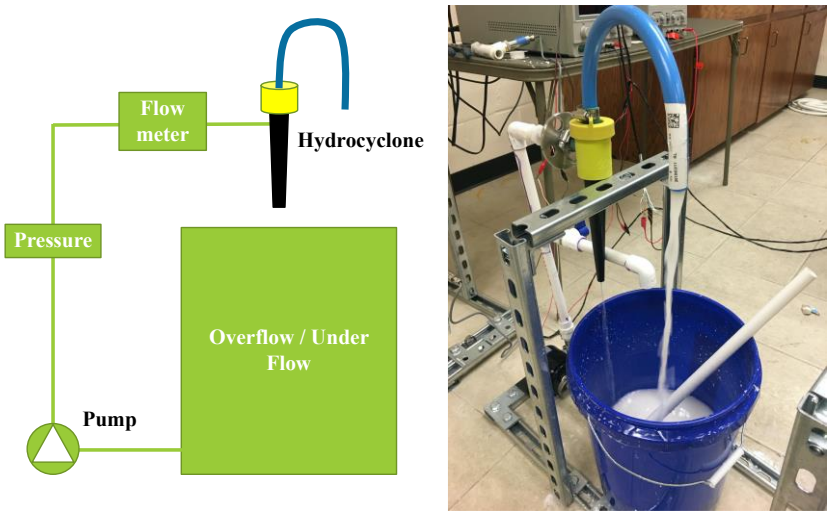

Figure 13. Compact hydrocyclone setup - to study the effect of piping size

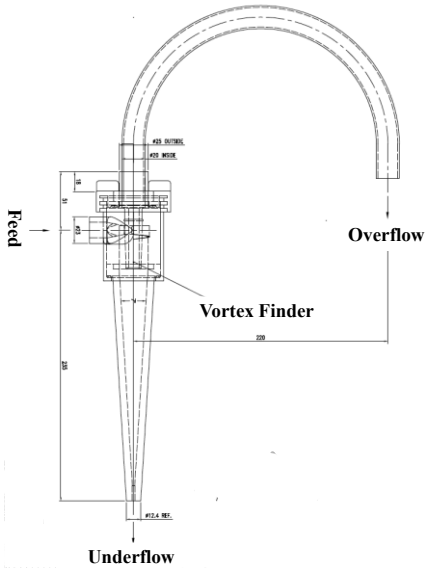

Figure 14. Schematic of the FC25-7 hydrocyclone

The hydrocyclone came with variety of vortex finder and spigot diameters which needed to be inserted and replaced considering the nature of the slurry in the setup, Fig. 15. Custom made3D printed vortex finders were designed and manufactured in house using a 3D printer to make changes in the design of the hydrocyclone more than what it was originally provided by the manufacturer company.

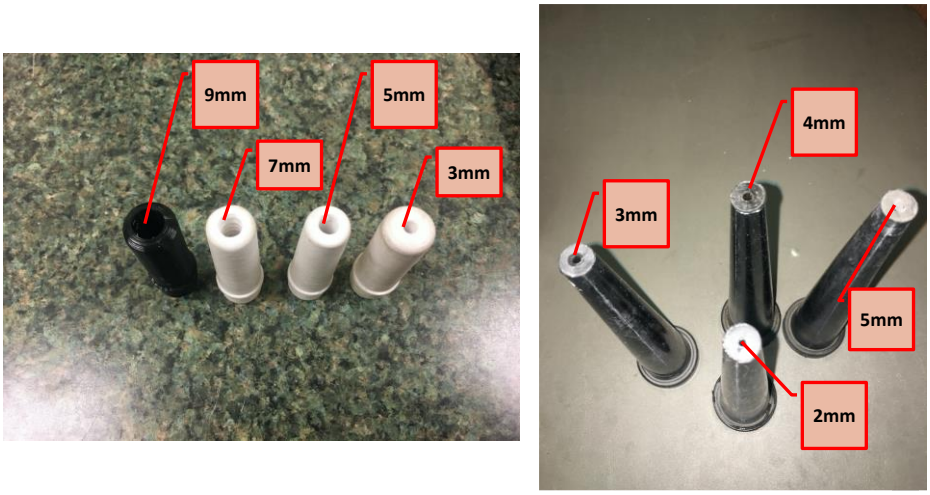

Figure 15. Variety of vortex finder and spigot diameters - provided by the manufacturer.

As described in the previous sections, the separation happens based on the density of each phase using the centrifugal force that is being created using the flow velocity. For the purpose of this study, there are 2 main different slurries including water and vegetable oil as the liquid phase and 2 different solid particle powder materials as the solid phase. The following will describe the combination of each slurry and how they have modeled the actual ice and brine slurry.

In the final setup, the mixture of ice, brine and ICL will be present. Density of each phase will be approximately 0.9, 1.2 and 0.8 g/cm^3, respectively. To validate the model, considering the very low temperature nature of the proposed method, it was decided to first simulate the experiments with other materials with similar density range in room temperature. Water as an available and relatively cheap material was chosen as the liquid phase in the mixture. The density of the water in our model experiments considered to be 998 kg/m^3. Glass microbeads with a density of 2600 kg/m^3 and type of PCM[6] named Paraffine wax with a density of approximately 900 kg/m ^{3} was chosen as heavy and light solid particle for the mixture.

2.3.2. Results and discussions

Water-based slurries were made using the MPCM and glass microbeads with different mass fractions to model the original slurry and investigating the separation efficiency of the hydrocyclone setup. Created glass microbead slurries are presented in Table 1.

[6] Phase Change Material

Table 1. Water-glass microbeads slurries information

Materials	Density (kg/m^3)	5% wt[7]	7% wt	9.2% wt
Water	998	3790 g	3790 g	3790 g
Glass microbeads	2600	217 g	304 g	400g

The water-glass microbeads slurries were prepared separately and have been added to the setup afterwards. Considering the density difference of the 2-phase involved, the slurry needed to be manually stirred during the experiment. Flow rates between 0 to 4.5 GPM was provided by the setup (less than the maximum flow rate of the pump considering the losses during the pipes) and separation efficiency was recorded for each different slurry. As it was discussed in the previous section, the hydrocyclone package included variety of VF[8] and Spigot diameters, that would help to find the best combination for each specific slurry to get the highest separation efficiency. Every possible combination of VFs and spigots for each slurry in the experiment were studied, and for the water-glass microbeads, the 9 mm VF and 2 mm spigot combination works the best among all the other options. The reason to this finding is that for the current slurry in which the higher density glass microbeads want to discharge through the underflow, the smaller the outlet the lower the amount of water will be and therefore the higher amount of microbeads will exit the underflow. Likewise, the 9 mm VF will make the way easier for the lighter phase (water here) to discharge through the overflow. Reducing the size of the VF or increasing the Spigot diameter will decrease the separation efficiency.

Figure 16 describes the experiment results for the water and glass microbeads slurries with different mass fractions in the hydrocyclone separation setup. Each experiment was carried out three times to eliminate the human error factor to a considerable extend. The reported results are the mean values of the carried-out experiments and it can be indicated that all the experiments results were in a margin of ±5% throughout the experiments. Figure 17 shows the mass percentage of Solid particles in overflow discharge to be zero at every flow rate. This indicates that the separation of at least one phase is happening inside the hydrocyclone setup.

7 Mass Percentage

8 Vortex Finder

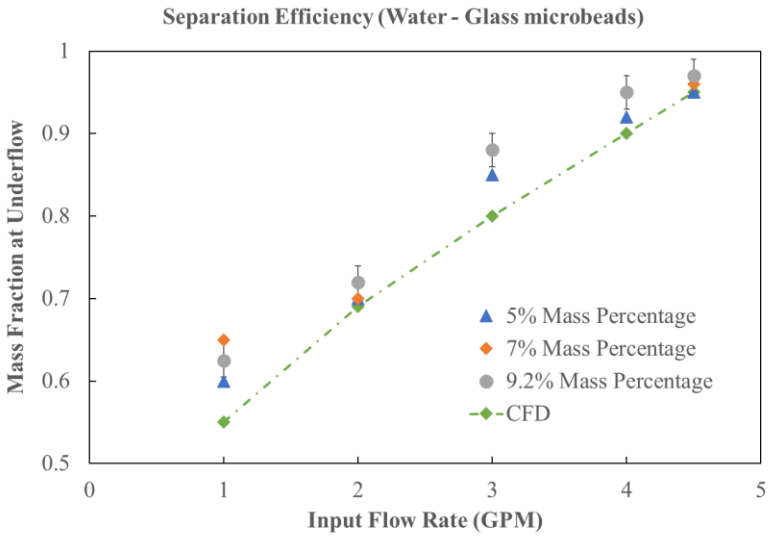

Figure 16. Water-glass microbeads separation ratios

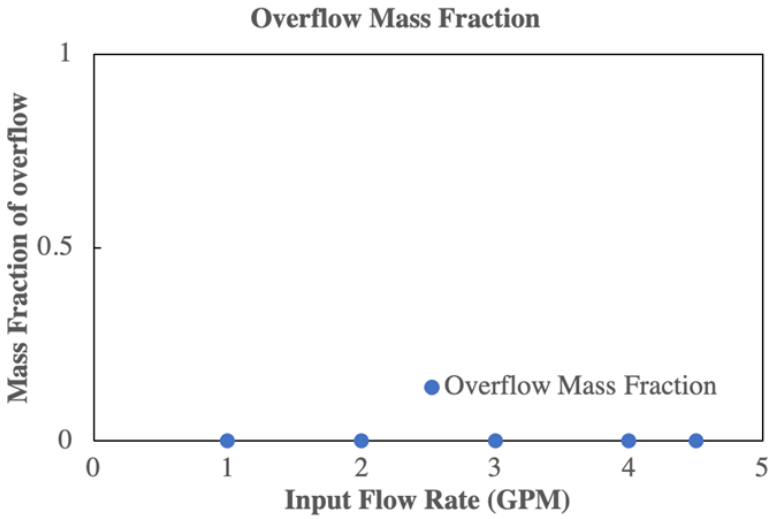

Figure 17. Overflow discharge - mass fraction of solid particles

The trend in which by increasing the flow rate separation ratio increases is proven in all the mass percentages. However, the 9.2% wt will have the highest separation ratio of 0.96. These numbers were calculated by weight measurements of the underflow materials using a laboratory scale. The plot compares the experimental results with those of the CFD simulation and they have been found to be in good agreements.

Increasing the mass fraction of the slurry higher than 10% will cause clogging in the hydrocyclone. Of course, the Spigot diameter can be increased to avoid clogging but as it was

mentioned before increasing the Spigot diameter will decrease the separation ratio which is not desirable.

In the case of mixing the PCM paraffine wax with water, the heavier phase will be water with 998 kg/m^3. The slurry needs manual stirring since the PCMs are not easily dilute in water. As an effort to make a better slurry of PCM and water, an ultrasound/heater device was utilized to agitate[9] and warm up the slurry up to around 60°C where the PCMs start to melt and better mix with water, Fig. 18. However, although the slurry became more blended after using the ultrasound and heater, water and PCMs still got split after a few minutes therefore the need for the manual stirring was reduced but not completely eliminated.

Figure 18. Ultrasonic & Heater utilized to better mix the PCM and water slurry

Similar to the previous water-glass microbeads slurry, the PCM and water slurry is made separately and is being added to the setup afterwards. 2 different mass fractions for this particular slurry were chosen to be 3% wt and 5% wt. Table 2 describes the properties and information of each slurry.

Table 2. PCM and water slurry information

Materials	**Density (kg/m^3)**	**5% wt**	**3% wt**
Water	998	4000 g	4000 g

[9] Using sound waves.

PCM (Paraffine wax)	900	199 g	122 g

The slurry was run through the setup with flow rates between 0 to 5.2 GPM provided by the Iwaki pump. Our experiment results indicate that in the case of water-PCM slurry, since the densities of each phase is relatively close, the hydrocyclone is not capable of separating them efficiently. It is worth noticing that considering the densities of each phase, it was expected to have PCM discharged into the overflow outlet. No matter what the flow rate was or what kind of mass percentage of Water-PCM slurry was running through the setup, both phases in overflow and underflow discharges were always present. Table 3 describes each outlet discharge with specific mass of the phases.

Table 3. Overflow and Underflow discharge information for PCM and water slurries

Concentration	**Flow Rate**	**Initial PCM**	**Overflow Discharge**	**Underflow Discharge**	**PCM at Overflow**
5% PCM	5.2 GPM	199 g	5.1% PCM	~ 0.5% PCM	101 g
5% PCM	2.6 GPM	199 g	4.3% PCM	2% PCM	68 g
5% PCM	1.3 GPM	199 g	4.2% PCM	2.1% PCM	60 g
3% PCM	5.2 GPM	122 g	3.05% PCM	~ 0.4% PCM	71 g
3% PCM	2.6 GPM	122 g	2.9% PCM	~ 1% PCM	66 g
3% PCM	1.3 GPM	122 g	2.5% PCM	1.3% PCM	49 g

The latter table describes quantitatively that by increasing the flow rate in both 3% wt and 5% wt slurries, the overflow PCM discharge or the separation efficiency will increase. Also, while increasing the flow rate, the underflow discharge PCM mass fraction will decrease. However, the overall separation efficiency of the hydrocyclone setup for the water-PCM slurry would not exceed approximately 60%, which is drastically lower compared to what the experiment results showed in the case of the Water-Glass microbeads slurry. Figure 19 compares the separation efficiency of both 5% wt and 3% wt PCM-water slurries in the hydrocyclone setup. Each experiment was carried out three times to minimize the random error. The reported results are the mean values of the carried-out experiments and it can be indicated that all the experiments results were in a margin of ±5% throughout the experiments.

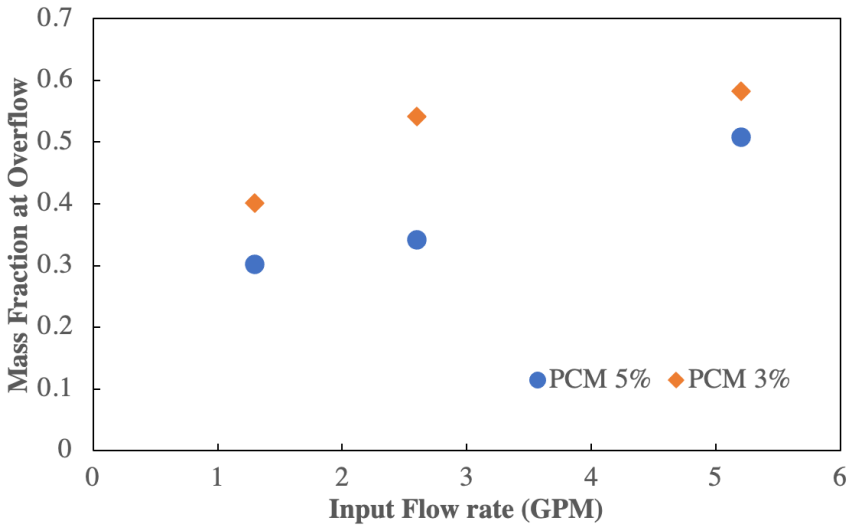

Figure 19. PCM-water slurry separation ratio

After running experiments for each slurry separately, a series of experiments were conducted which included both PCM and glass microbeads as the solid phase. Table 4 describes the specific information for the new slurry.

Table 4. PCM, Glass microbeads and water slurry information

Materials	Density (kg/m^3)	Mass	Mass Percentage
Water	998	3790 g	88.1%
PCM (Paraffine wax)	900	116 g	2.7%
Glass Microbeads	2600	400 g	9.2%

The latter slurry was run through the hydrocyclone setup with flow rates between 0 to 4.5 GPM provided by the pump. The Pressure of the flow was monitored using a pressure transducer which sends the recorded signals to an Arduino electronic board in which the signal is being translated by a code that was generated for this purpose and recorded on the computer to be 24.01 psi throughout the experiment. Figure 20 shows the separation ratios for the PCM-Glass Microbeads-Water slurry in the hydrocyclone setup.

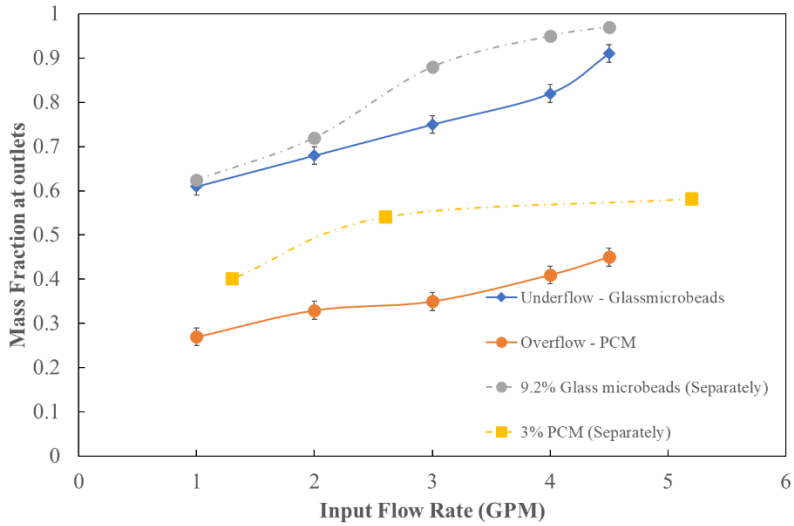

Figure 20. Separation ratio for PCM and glass microbeads slurries

Each experiment was carried out three times to eliminate the human error factor to a considerable extend. The reported results are the mean values of the carried-out experiments and it can be indicated that all the experiments results were in a margin of ±5% throughout the experiments. According to the experimental results, as shown in Fig. 19, the increasing trend for separation ratio is still in place when running the complete PCM and Glass microbeads slurry through the hydrocyclone setup and ratios around 0.9 is achieved for the underflow discharge where it was expected to see glass microbeads. It is worth noticing that when comparing the results for the latter slurry separation ratios with what it was before, while running slurries separately, in both underflow and overflow discharges, lower separation ratios for the complete PCM-glass microbead slurry was reported. This means that after mixing both types solid particles with water and running them through the hydrocyclone, it was experiencing reduction in separation ratios. In addition, while running the complete slurry, the same problem was encountered which was raised in running the PCM slurry through the hydrocyclone in which the device was not capable of separating the PCMs fully from the water due to the densities of both phases being very close to each other.

After evaluating the hydrocyclone experiment results, it was concluded that the hydrocyclone is not the best device to perform the separation stage of the ZDL freeze desalination method. The uncertainty of the hydrocyclone to separate close density phases will make troubles while separating ice and ICL which eventually make the desalination product contaminated and not meeting the universal standards of desalinated water. Therefore, it was decided to study another

method of separation using a hydraulic wash column which is explained extensively in Chapter 3.

3. Numerical and Experimental Study on Hydraulic Wash Column

A comprehensive numerical and experimental study is performed on the behavior of hydraulic wash columns as a continuous solid-liquid separation method. A brief background and literature review is presented to better understand the principles of wash columns and previous studies in the literature. The numerical model and its results is explained in details followed by the results of the most current efforts that have been done in validating the model in an experimental setup. Considering that the work is still ongoing in the experiments, suggestions have been provided for the future work.

3.1. Background and literature review

In order to meet the desired product purity, an effective phase separation and possibly further purification of the crystal phase must be achieved in the downstream separation unit. For this purpose, wash columns have been developed, which combine a virtually complete product-residue separation with an efficient countercurrent washing action. Three types of industrial wash columns are distinguished by the different mechanisms applied to trans- port the crystals: gravity, hydraulic and mechanical columns [8].

In the first type, the crystals settle under gravity into a loosely packed downward moving bed and the mother liquor leaves the column via the overflow. A slowly rotating agitator ($\lesssim 0.035$ s^{-1}) covers the whole length of the wash column and serves to prevent agglomeration and/or channeling in the bed. The production capacity of gravity wash columns does not exceed 0.4 $kg/m^2.s$. The residence time of the crystals may amount to several hours due to the large column height (6-8 m) [8]. In the second type, a densely packed crystal bed is transported by hydraulic pressure. The mother liquor flows through the top section of the crystal bed and leaves the column via filters which are positioned either in separate filter tubes or in the column wall. From a scale-up point of view the version with separate filter tubes, known as the TNO-Thijssen column, is favorable. The product throughput can be as high as 2.8 $kg/m^2\ s$. The residence time of the crystals in the compact equipment (height: 1-1.5 m) is in the order of 10-15 min [9].

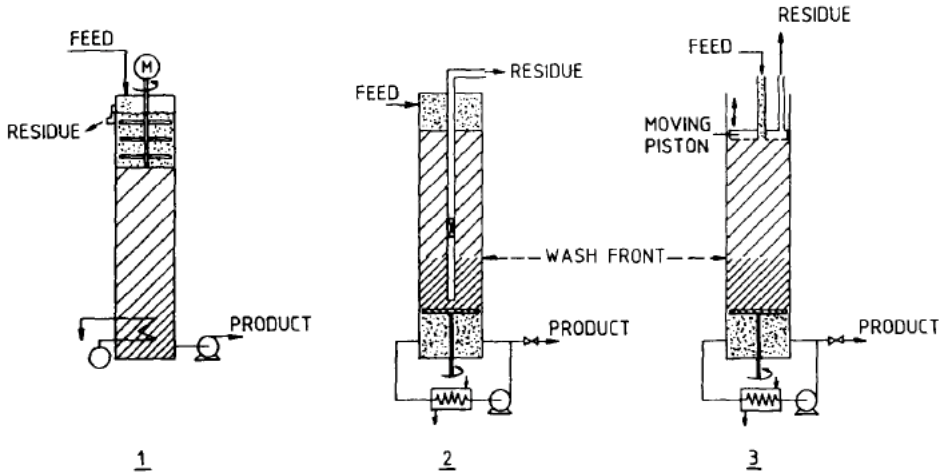

Figure 21. (1) Gravity, (2) hydraulic and (3) mechanical wash column types [8]

In the third type, a densely packed crystal bed is transported by a mechanical force created by a moving piston or a rotating screw. The mother liquor leaves the column via pores in the mechanical device. Similar to the hydraulic type, the maximum throughput of mechanical wash columns is limited to 2.8 $kg/m^2\ s$, the height amounts to 1-1.5 m and the residence time of the crystals is about 10-15 min [9].

At the bottoms of all three column types the product crystals are molten. A major part of the molten product is withdrawn from the bottom section and the remainder ascends in the column thus providing a countercurrent washing action. The wash liquid (partly) crystallizes on the descending cold crystals. In the densely packed hydraulic and mechanical wash columns complete recrystallization of the wash liquid produces a sharp wash front. This wash front represents the border line between impure mother liquor and (nearly) pure wash liquid and it marks steep gradients in porosity, concentration and temperature [8], [9]. The purity of the crude crystals descending in the wash columns is expected to increase due to (1) displacement of the mother liquor, (2) washing of the liquid layer adhering to the crystals, (3) crystallization of pure wash liquid on the cold crystals, (4) sweating of the crystals in contact with the hot wash liquid and/or adiabatic recrystallization of the crystals [9].

The contribution of the individual purification mechanisms depends on the contact time between the crystals and the wash liquid and on the morphology and composition of the crude crystals. In gravity wash columns with long contact times, recrystallization and sweating may result in the removal of incorporated impurities (solid solutes) and included impure mother

liquor. In hydraulic and mechanical wash columns, however, the contact times are short and removal of impurities from the inside of the crystals is less likely to occur [8].

Jansens et al. [8], performed an experimental and mathematical study on the purification process in packed bed wash columns. Their developed model can be used to calculate concentration, temperature, and porosity profiles along the column axis and to predict the effect of operating conditions on the product purity. In a series of experiments, the temperature profiles at the wash front and the product purity were monitored in steady-state operation under various operating conditions. The experiments were performed with a pilot plant, TNO-Thijssen type, hydraulic wash column. The height of the wash column was 1 m, and it had an internal diameter of 0.156 m. The column contained six filter tubes with an outer diameter of 0.02 m. Results from this study showed that the product purity and the temperature profiles at the wash front are independent of the product throughput and the wash front height in the ranges studied. Consequently, the maximum product throughput of hydraulic wash columns depends only on the transport force balance and is not limited by purification requirements.

A model was developed by Bruinsma et al. [10], to simulate the dynamic behavior of a hydraulic wash column. The model combined slurry properties, wash column dimensions, and input process conditions to predict the length of the crystal bed and the wash section, the pressure at the top and the bottom of the bed, and the product and residue flow rates. The dynamic model was validated in a pilot plant with a pressure-dependent feed pump that was influenced by the pressure in the wash column. In the standard pilot plant containing a 70L crystallizer and a 15.6 cm diameter wash column the validation experiments were obscured by the interaction between the crystallizer and the wash column. Even though the outputs were not predicted exactly, but the general trends in the length of the crystal bed and the wash front height were followed satisfactorily.

A feedback control system with two control loops was used to keep both the length of the bed and the wash front at desired setpoint values. Simulations with this extended model showed that the levels can easily be controlled for 10% step changes in the crystal content of the feed. Large overshoots occurred when the crystal content increases more than 10%. However, no instability problems occurred, and the wash column can still be operated as long as the crystal fraction is between 0.06 and 0.30. When the set point for the length of the bed or the length of

the wash front is changed, the control system was able to adjust the length of the wash section and the length of the bed to these changes.

Controlling the flow in the wash column is a bit tricky! It takes a huge lot of effort to finally make the flow right and have the washing loop work and separate the washed ice from the column. The appropriate operating conditions that lead to a successful washing were proposed in Qin et all. [11]. They have studied a mechanical wash column that was made of a Perspex cylinder with an inside diameter of 80 mm and height of 500 mm. The ice slurry was produced with a laboratory scale scraped surface heat exchanger. After aging for a given time, the ice slurry was manually filled into the wash column, and the ice bed was com- pressed using a mesh piston until it reached the 'ice bed line'. The compressing force was provided by weight(s) at the top end of the piston rod giving 0.1–0.5 kg/cm^2 pressures. An ice-free section of mother liquid above the mesh piston was produced after compression. This part of the mother liquid was then drained to allow the liquid level to be flush with ice bed surface. The mesh piston was kept in the wash column to maintain the pressure and prevent water rushing into the ice bed.

Wash operation may fail due to a number of problems, such as channeling, viscous fingering, and clogging etc. [11], [12]. An often-seen problem (an undesired phenomenon) was that a sharp, clear, horizontal wash front was not visible. Instead, the transitional region between the washed and the unwashed ice-layer was blurred or too large, or even worse — no washed ice-layer was produced. The reason seemed to be over-mixing of the washing water with the mother liquid. But careful observations (with the help of dye-tracer) showed that this might be attributed to two phenomena: channeling and viscous fingering. When the local ice bed progressively became loose during washing because of melting or ice being washed away, channeling occurred. Channels often appeared as a number of downward caves in root-like shape. Viscous fingering occurred when the wash front moved faster at some locations than others. Both channeling and viscous fingering occurred often in the vicinity of the column sidewall [12].

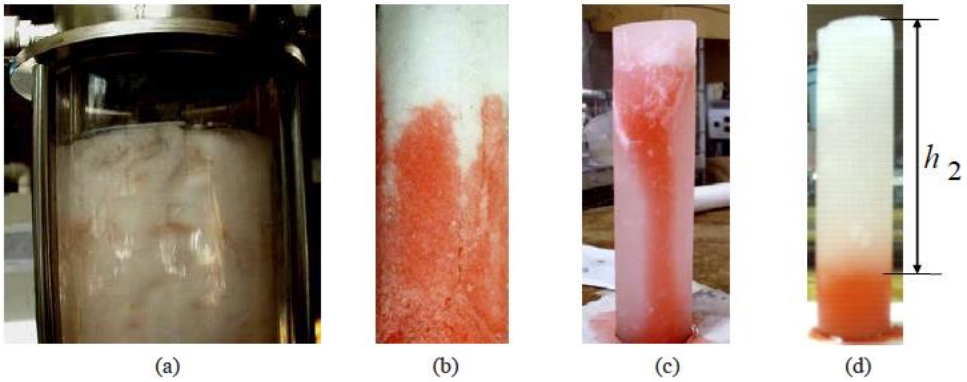

Figure 22. Phenomena found in wash columns [12], (a) channeling (b) beginning of viscous fingering (c) development of viscous fingering (d) a successful wash

Another potential problem is clogging in the ice bed resulted from over crystallization of ice in the porous ice bed. High concentration of the mother liquid with strong freezing point depression (FPD) will enhance this effect. Experiments in [10] & [11], also showed that it usually happened when the ripening time given to the ice slurry was insufficient. The 'premature' ice slurry perhaps contained a large number of very fine ice particles so that the permeability was poor. The situation became worse when the ice bed was over compressed, which also resulted in dead-end pores and liquid occlusion (liquid sack) inside ice lumps due to pressure-induced fusion of ice. Clogging of the ice bed prolongs the washing time and the ice close to the wall gradually melts and eventually leads to channeling near the wall.

3.2. Numerical study on hydraulic wash column

A small CFD model is presented to investigates the accumulation of the solid particles in a wash column, with the original lab scale dimensions (which will be discussed in section 3.3). The geometry and generated grids in ANSYS Fluent are shown in Fig. 23. The geometry has been created in Design Modeler feature in ANSYS Workbench and then imported to the Meshing area of the Workbench. The final grid was exported as a mesh file into Fluent for numerical calculations of the model. In Fluent, Continuity and Momentum equations were solved numerically.

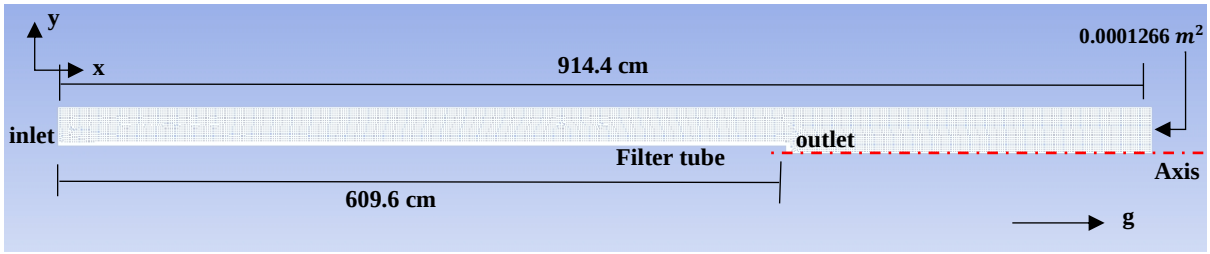

Figure 23. Wash column model geometry and computational grid

The slurry enters the column from the inlet, which is situated at the top plate, and due to the drag of the mother liquor, the particles are transported to the bottom parts of the column to form a packed bed. To simulate the brine-ice slurry, it was chosen for the mother liquor phase to have 1200 kg/m^3 and solid particles to have 920 kg/m^3 density. The setup is included an inlet at the top and an outlet at filter tube each by 0.0001266 m^2 surface area. The actual experimental setup (will be explained in section 3.3) has one inlet and two outlet filter tubes as well as one outlet at the bottom to extract the accumulated solid particles. Here the model is only simulating the accumulation of the solid particles and did not investigate the extraction. The area of the top and bottom plates is 0.004560 m^2, the length of the column is 914.4 cm, and the filter tube length is 609.6 cm.

The model is consisting of 10530 cells and has set up in a steady state, axisymmetric (the location of axis is shown in Fig. 21) and pressure-based solver with gravity in the positive x direction. A similar study of a wash column with half top and bottom diameter with 0.001140 m^2 surface area was modeled, Fig 24. This model has half diameter of the original simulation and it was generated to compare the effect of base diameter on separation efficiency and wash front. All the other dimensions are similar to the model with original dimension simulation. This model is consisting of 17406 cells. The results of both simulations will be discussed in detail after model description.

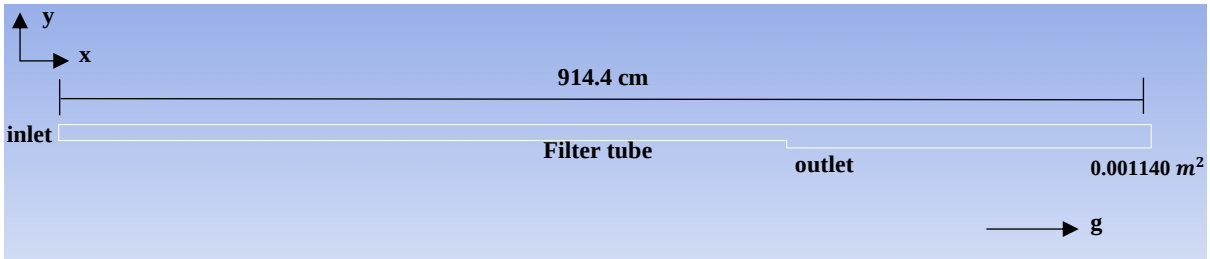

Figure 24. Generated geometry with half base diameter compare to the original setup

Considering the density of each slurry in the numerical model, and the range of cross-sectional flow velocities inside the column (from 0.5 m/s to 2 m/s), the Reynolds number was calculated to have a range from 8770 to 1.75×10^5. This Reynolds number range is clearly indicating that our flow is turbulent. To solve the governing equations for this model the turbulent k-epsilon model (2 eqn.) with standard wall functions for near wall treatments was chosen, Fig. 25. Also, to simulate the movements of the particles in the slurry, the Discrete Phase Method (DPM) was utilized.

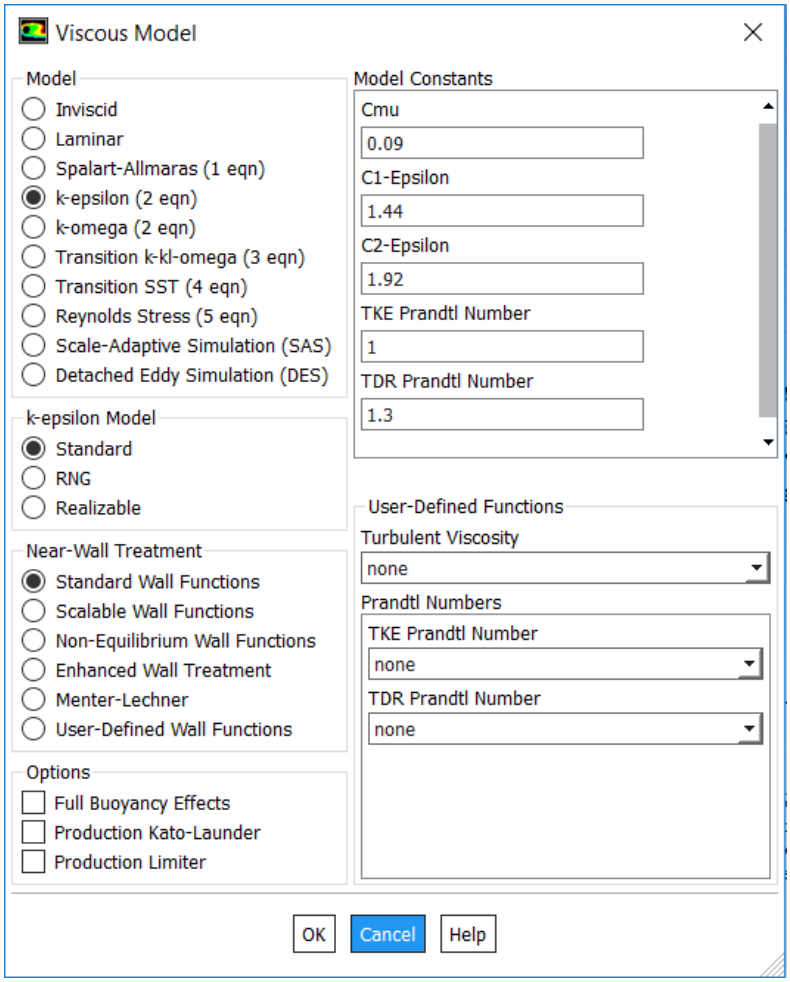

Figure 25. Configuration of the *k-ε* turbulent model in Fluent

For the DPM model, the unsteady particle track method was chosen with a 0.0005 s time step size. In all of the simulations, the 5% mass percentage of particles for the slurry is considered. The boundary condition at inlet is considered to be a velocity-inlet with different flow velocities from 0.5 m/s up to 20 m/s. The filter tube outlet is considered to be a pressure outlet with zero-gauge pressure. The no slip boundary condition is applied to all the other

boundaries in the simulation domain. The symmetry axis is located on the bottom side of the domain where it is exactly over the *x* axis.

The solution methodology is considered to be a Simple scheme pressure-velocity coupling, PRESTO! For pressure and Power law for the Momentum equations. In addition, First Order Upwind schemes was chosen to solve both turbulent kinetic energy and dissipation rate equations.

To better understand and discuss the results of the numerical simulation, there is the need to introduce zone definition in our model. The main goal of the CFD model is to determine the flow velocity and flow rate necessary for the column to be able to separate the particles and also create the packed bed at the bottom section. Therefore, 4 zones was introduced, each shows quarter of the domain that utilized to study based on the flow velocity and flow rate. Figure 26 shows the newly introduced zones in the domain. Each zone has 228.6 mm length. As discussed earlier, our objective is to find the optimum velocity to for the packed bed of solid particles in zone 4.

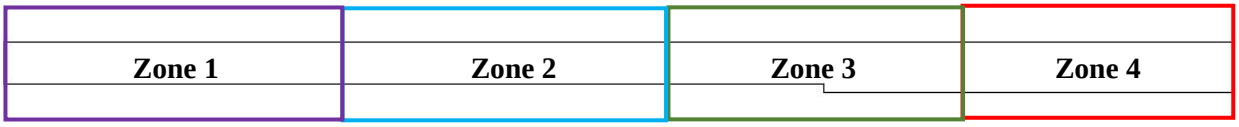

Figure 26. Introducing zones in the model, dividing the domain into 4 zones

Starting from a 0.5 m/s flow velocity, a series of calculation was conducted to investigate the position of the wash front[10] and separation behavior of the column. Figure 27 indicates that the accumulation of the solid particles starts to form a packed bed in zone 1 and the wash front resist to move towards the lower zones.

[10] The imaginary line that separates the packed bed from the mother liquor phase in the column.

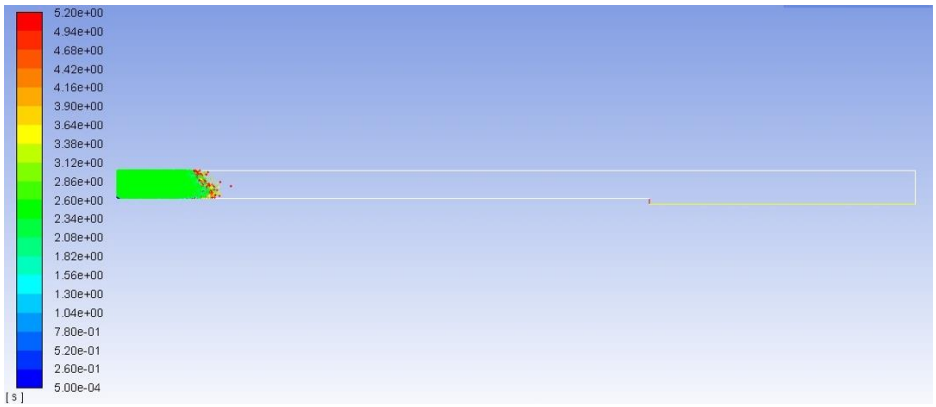

(a)

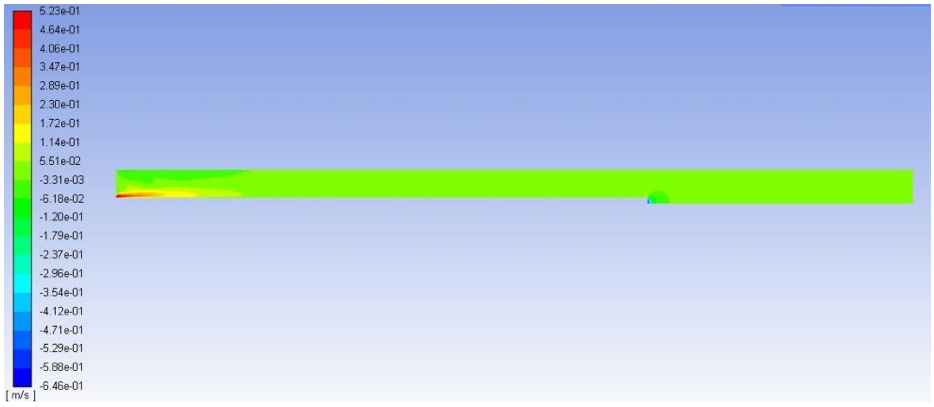

(b)

Figure 27. CFD results for 0.5 m/s flow velocity, (a) particle residence time (b) axial velocity contour

The particle residence time in Fig. 27a, indicates that particles tend to remain in zone 1 as the time goes by. This finding proves that to get the packed bed in the lower sections of the column there is a need to change the operating conditions. One of our operating conditions is velocity and the other one is the base surface area. First, moving forward with increasing the velocity and after that the effect of base surface area on packed bed position is discussed.

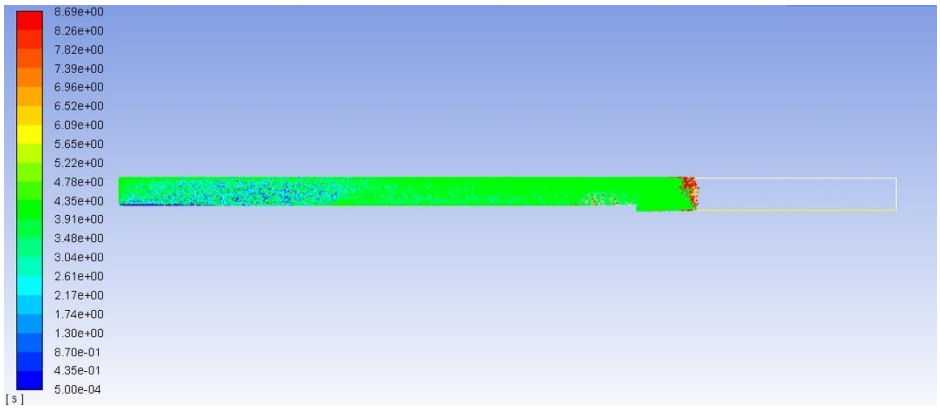

(a)

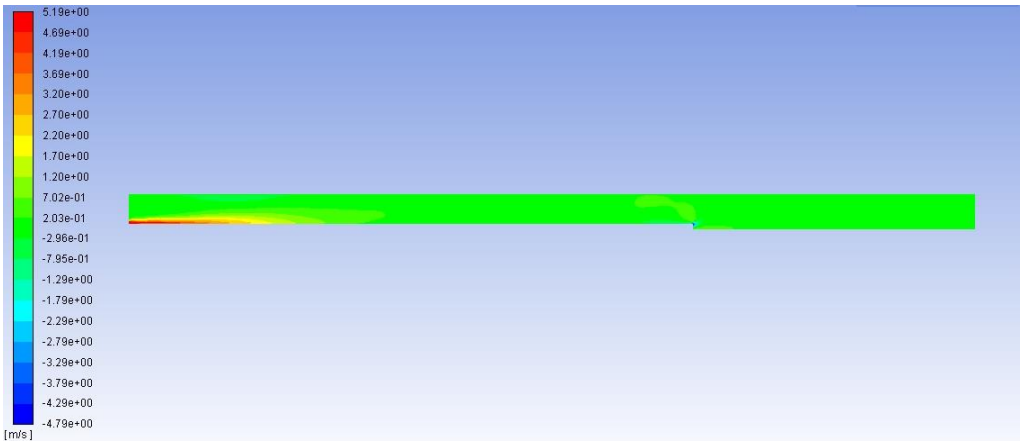

(b)

Figure 28. CFD results for 5 m/s flow velocity, (a) particle residence time (b) axial velocity contour

Increasing the inlet flow velocity to 5 m/s, our results shows that the packed bed starts to form in zone 3, Fig. 28a. The particles residence time for the case with 5 m/s inlet flow velocity proves that increasing the velocity helped moving the wash front towards the bottom section of the column, however, our desire zone is zone 4 so that the solid particles can be extracted from the bottom outlet, which has not been achieved with this velocity. Figure 28b shows the axial velocity in the domain for the case with 5 m/s inlet velocity. This contour indicates that the flow velocity into the domain is equal to the outlet velocity from the filter tube.

Other interesting finding from the particle residence time in Fig 28a, is that after the packed bed started to form, it has grown towards the top plate. Our results indicate that by increasing the time, the packed bed will not move towards the bottom plate and therefore it is necessary to increase the flow velocity to force the packed bed to form in the lower zones.

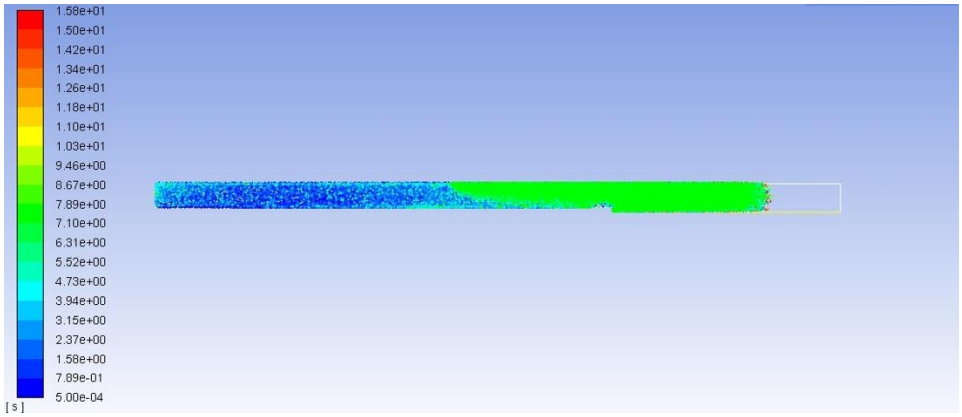

(a)

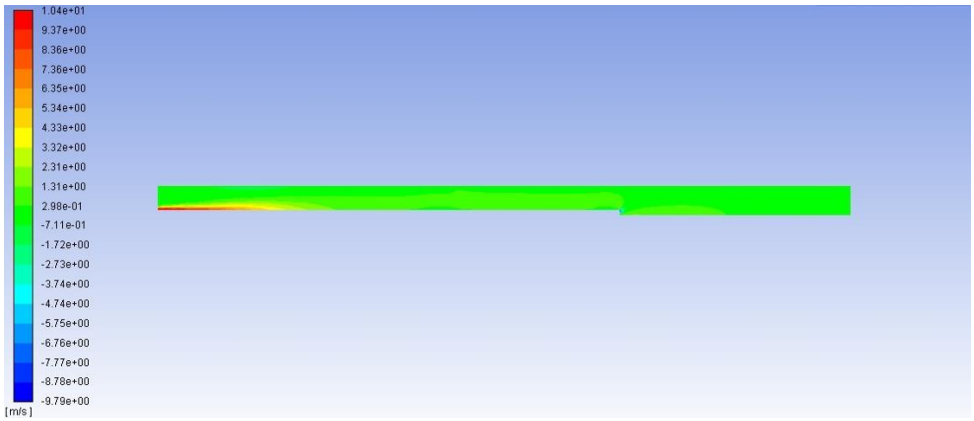

(b)

Figure 29. CFD results model for 10 m/s flow velocity, (a) particle residence time (b) axial velocity contour

By increasing the inlet flow velocity to 10 m/s, the simulation results indicate that the packed bed of solid particles starts to form between zone 2 and zone 1 and grows towards the top plate. The particle residence time in Fig. 29a shows that the wash front starts to move upward, and the solid particle packed bed will not move towards the bottom plate of the column. Now the question is how much increasing in the inlet flow velocity is meaningful? Does it worth it to go even higher? In reality, there should be a huge, powerful, and definitely expensive pump to provide these kinds of flow velocities and flow rates. The answer to the above question will depend on the operating conditions and available expenses for the project. However, here it is intended to find the theoretical flow velocity and therefore, higher flow rates were assigned to achieve the optimum operating condition.

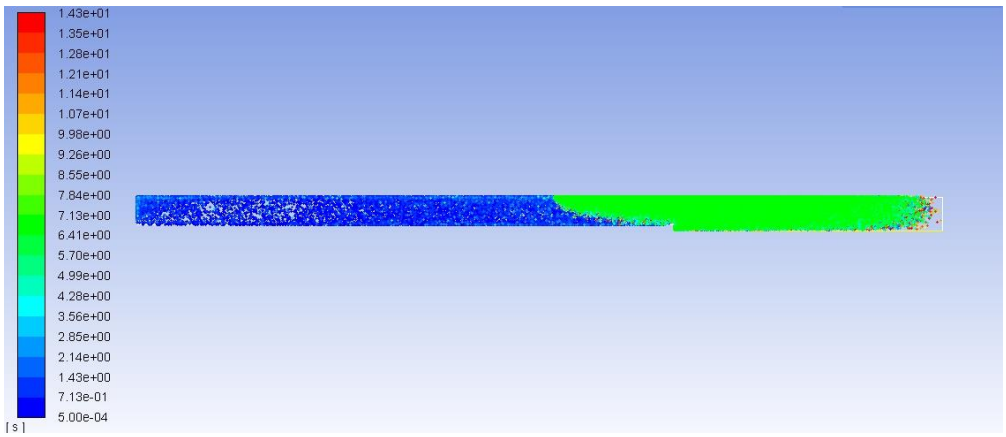

(a)

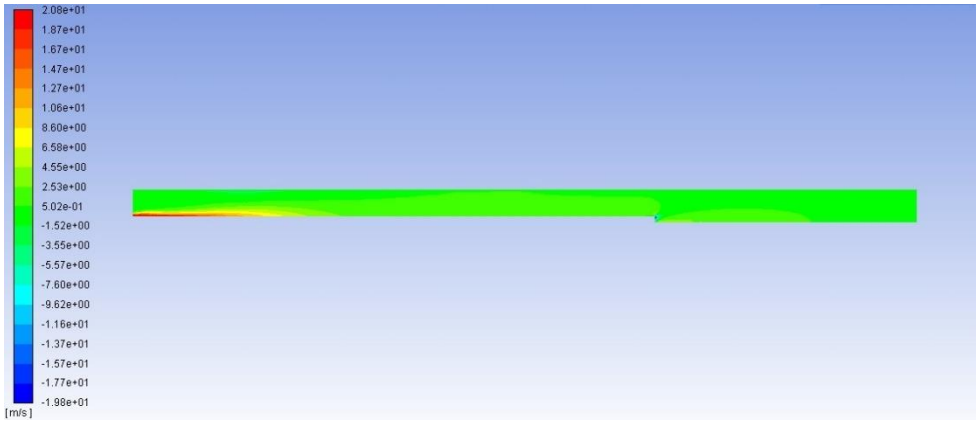

(b)

Figure 30. CFD results for 20 m/s flow velocity, (a) particle residence time (b) axial velocity contour

Finally, by increasing the inlet flow velocity to 20 m/s, the packed bed in the column started to form in zone 4, near the bottom plate and the particle residence time in Fig. 30a shows that, as the time goes by, the solid particles tend to move towards the bottom plate and therefore the optimum velocity for the inlet flow is find out to be approximately around 20 m/s. As discussed before in this section, there is another operating condition that needed to study the effect of it on the separation behavior and the position of the packed bed or wash front.

As it was shown in Fig. 25, an alternative model was developed with a half base diameter compare to the original design. The model was studied with inlet flow velocities from 5 to 15 m/s and the results will be discussed in the following. The main goal of this latter numerical study is to investigate the effect of column base diameter on the packed bed formation and wash front position.

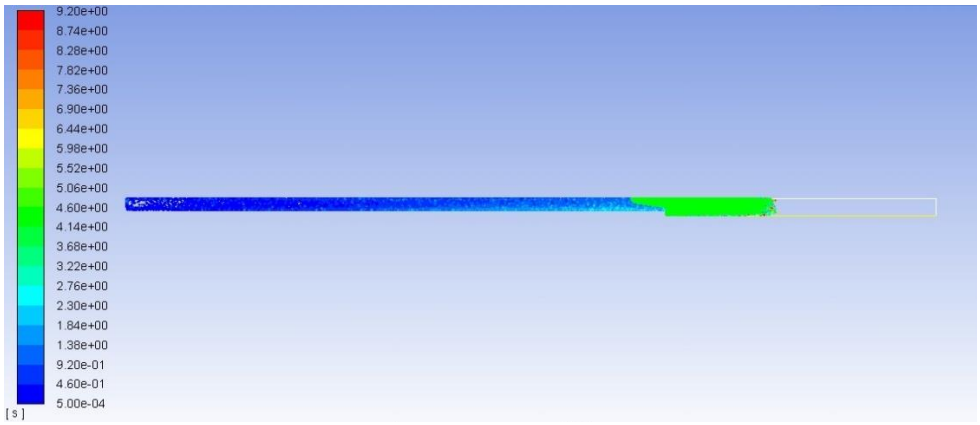

(a)

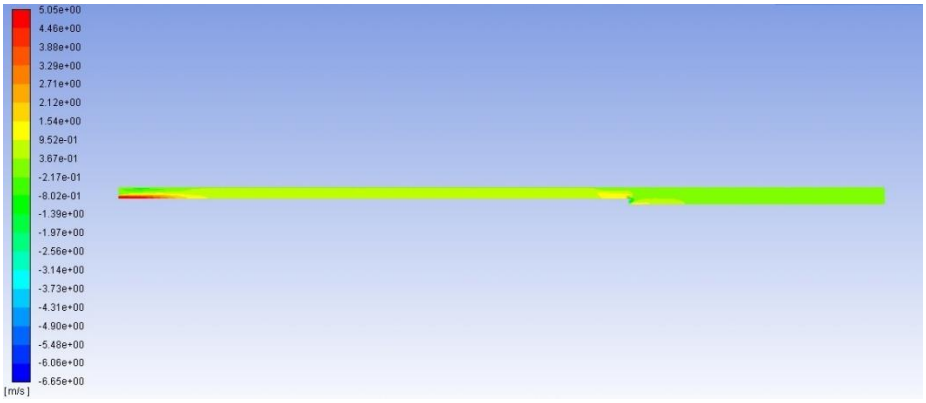

(b)

Figure 31. CFD results for 5 m/s flow velocity and half base diameter, (a) particle residence time (b) axial velocity contour

As it is shown in Fig 31a, the particle residence time indicates that the packed bed is initiated in zone 3 and has started to build up towards the top plate and the particles resist to move towards the bottom plate. Comparing the position of the packed bed with the case of the original dimensions, it could be clearly observed that the packed bed has been pushed a bit towards the bottom plate but obviously it has not been sufficient to form the bed in zone 4 near the bottom plate.

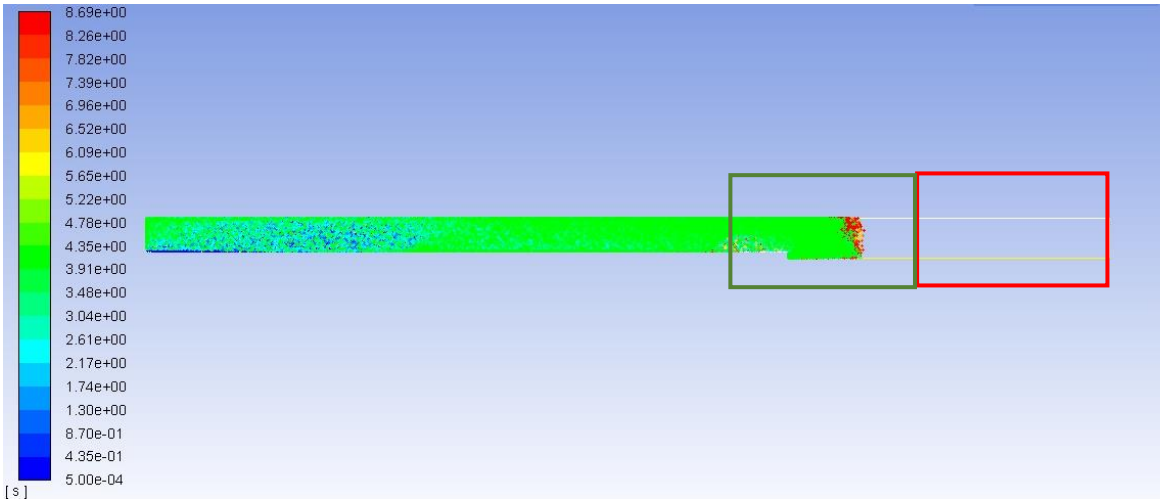

(a)

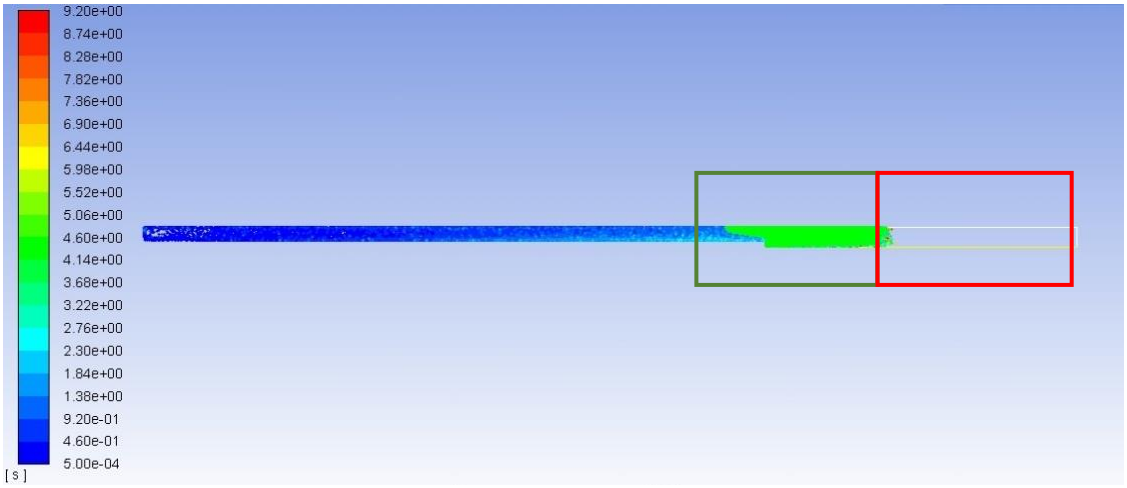

(b)

Figure 32. Comparison of packed bed position, 5 m/s inlet flow velocity, (a) original model (b) half base diameter model

By increasing the inlet flow velocity to 10 m/s as it is shown in Fig. 32, the position of the packed bed formation has not moved any further towards the bottom plate. Figure 30a shows the particles residence time in this case and indicate that the particles tend to form the bed in zone 3 and accumulate towards the top plate. Comparing the results from the case with original dimensions with this latter one, it can be observed that the position in which the packed bed is formed is closer to the bottom plate and in zone 4, for the original dimension model, Fig. 33.

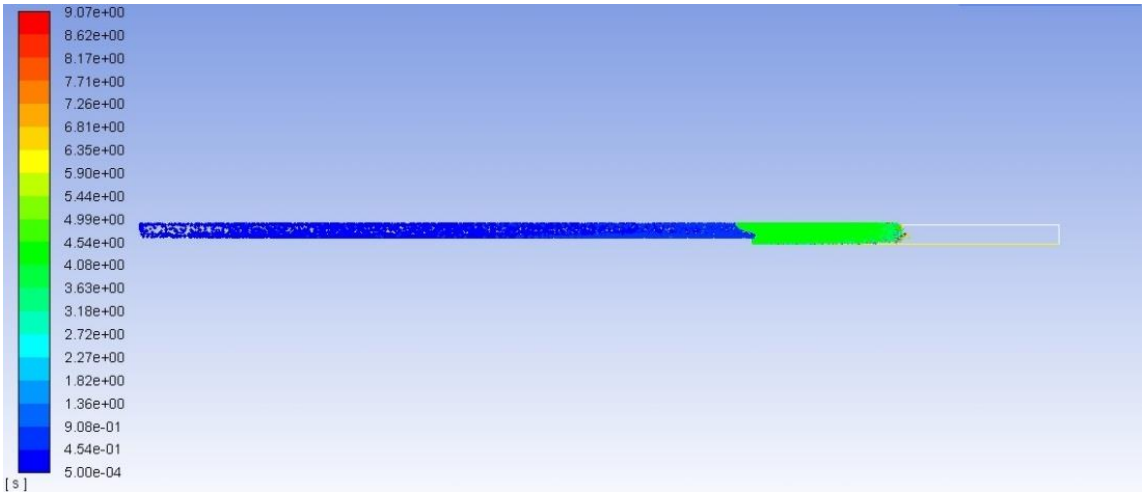

(a)

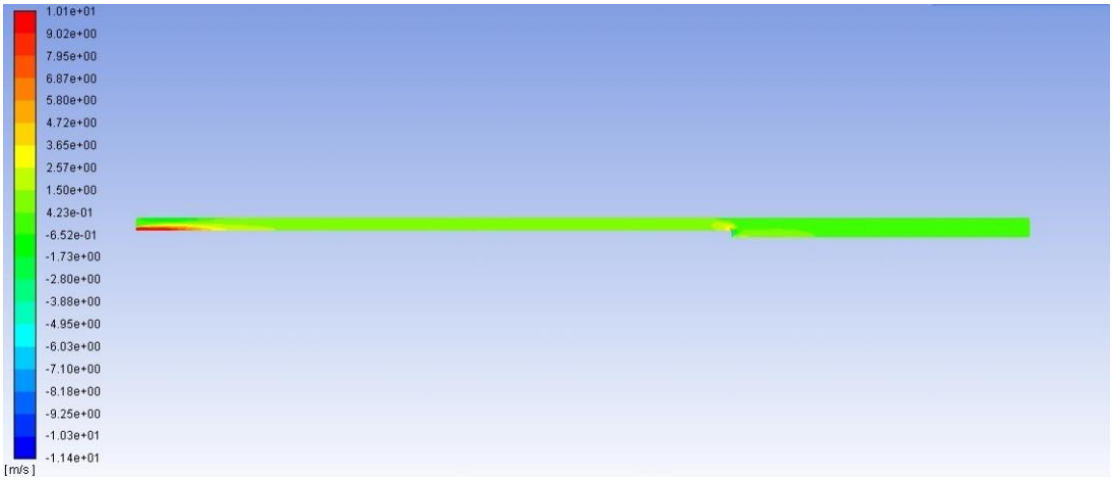

(b)

Figure 33. CFD results for 10 m/s flow velocity and half base diameter, (a) particle residence time (b) axial velocity contour

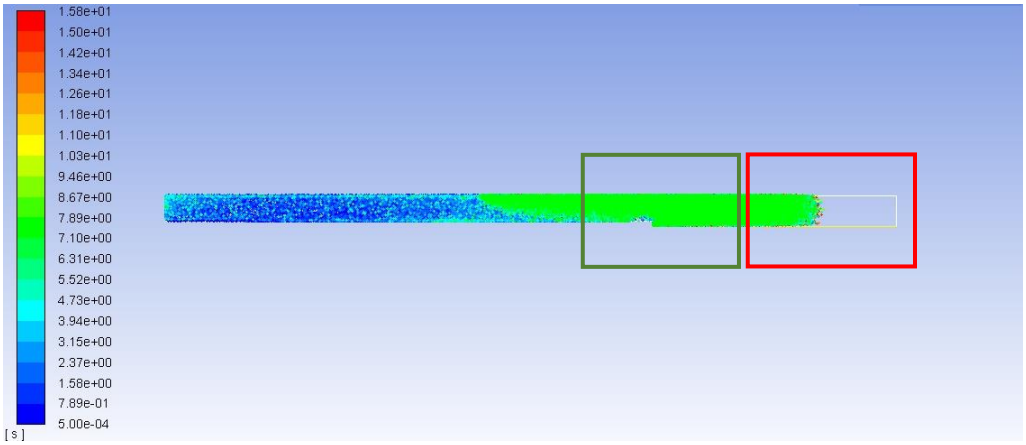

(a)

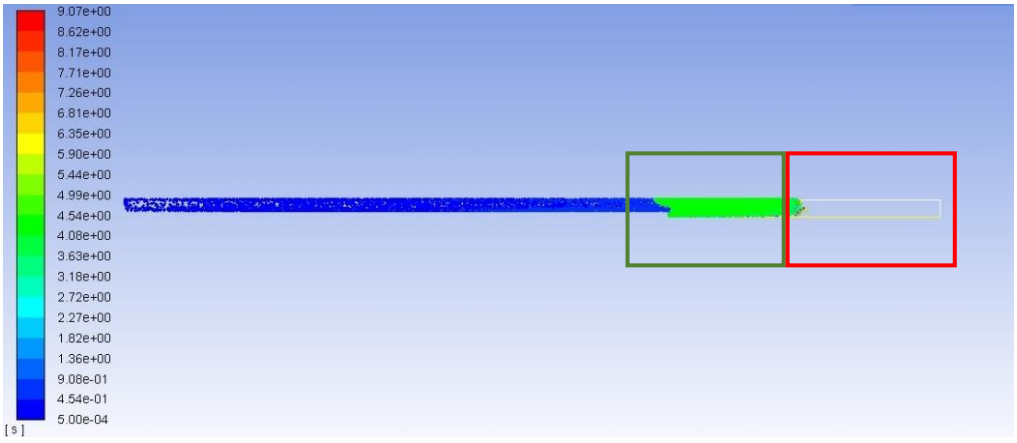

(b)

Figure 34. Comparison of packed bed position, 10 m/s inlet flow velocity, (a) original model (b) half base diameter model

To find the optimum inlet flow velocity, the inlet flow velocity was increased to 15 m/s. Figure 35 shows the results of this latter case.

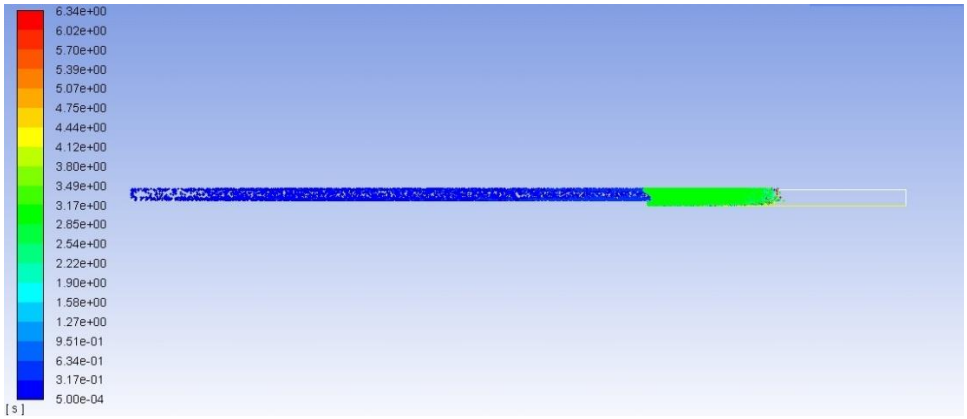

(a)

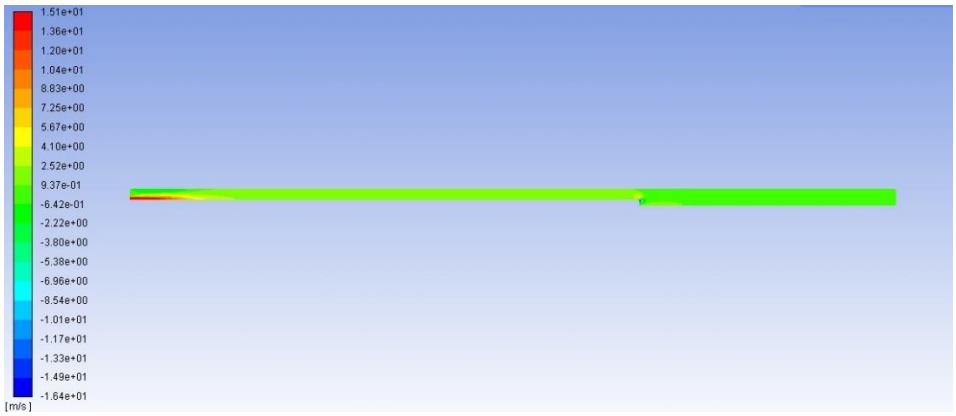

(b)

Figure 35. CFD results for 15 m/s flow velocity and half base diameter, (a) particle residence time (b) axial velocity contour

Surprisingly, the increase in the inlet flow from 10 to 15 m/s did not help the packed bed to form anywhere near zone 4 and bottom plate. The particle residence time results in Fig. 35a indicates that the packed bed starts to form in zone 3 and goes on to build up towards the top plate. The next section will discuss the experimental study on hydraulic wash columns. In this study, a lab scale hydraulic wash column was designed and manufactured and the setup was tested with different materials. The results from the latter experiments are discussed as well.

3.3. Experimental study on hydraulic wash column

As a final step towards studying the separation of solid liquid slurries, a lab scale hydraulic wash column was designed and manufactured. As it was discussed in section 3.1, there are 3 types of wash columns known as gravitational, mechanical, and hydraulic. All types are

separation units with almost similar mechanism in which the filtration happens in a column and pure extracted product can be discharged from either top or bottom. Now the question is which one would serve the best for our purpose. To answer this question, it is worth considering that in the gravitational wash column takes at least about 6-8 hours to form the packed bed and also the wash front is not clear and sharp. In addition, in the case of the mechanical wash columns, there is the need for the mechanical force to push the slurry down the column and form the packed bed. All of these limitations are not desired in our case and an alternative solution is needed to for our model. Therefore, there is only one remaining option which is hydraulic wash column.

Based on the literature review that has been presented in section 3.1, a hydraulic wash column was designed and built. However, to make this wash column unique and also applicable to our purpose and limitations, a few modifications were made to the common hydraulic wash columns which are known as TNO-Thijssen type. The modifications will be discussed later in this section. The schematic of the hydraulic wash column is presented in Fig. 36.

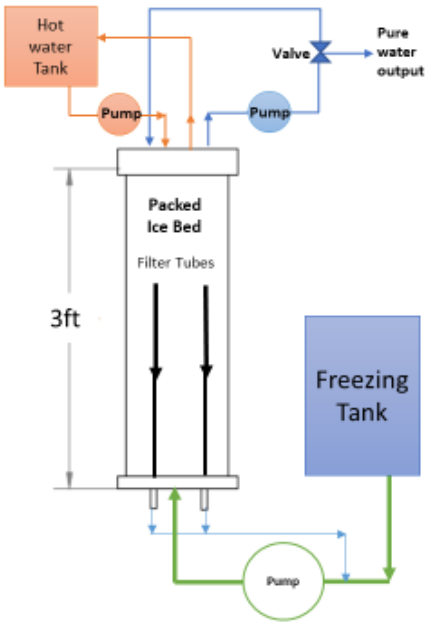

Figure 36. Schematic of the hydraulic wash column setup

As it is shown in Fig. 33, the wash column is located after the freezing tank where the ice crystals are created when the brine and ICL come in direct contact. The crystals among with the brine and ICL remaining run through a pump which accelerates the flow velocity to create

the necessary drag force inside of the wash column. After entering the column, the drag and gravity force take the slurry upwards and separation occurs when the liquid phases start to drain through the filter tubes. A brass custom made coil is located at the top section of the column in which water runs with the help of a pump from a tank. The water inside the coil gets in contact with a portion of the ice packed bed and helps the ice particles to get discharge as pure water through the outlet at the top. A loop of pure water then will be run through the column from an inlet on top plate to wash to packed bed and help crystalizing any contaminant present in the packed bed. Figure 37 describes each loop and materials in the setup.

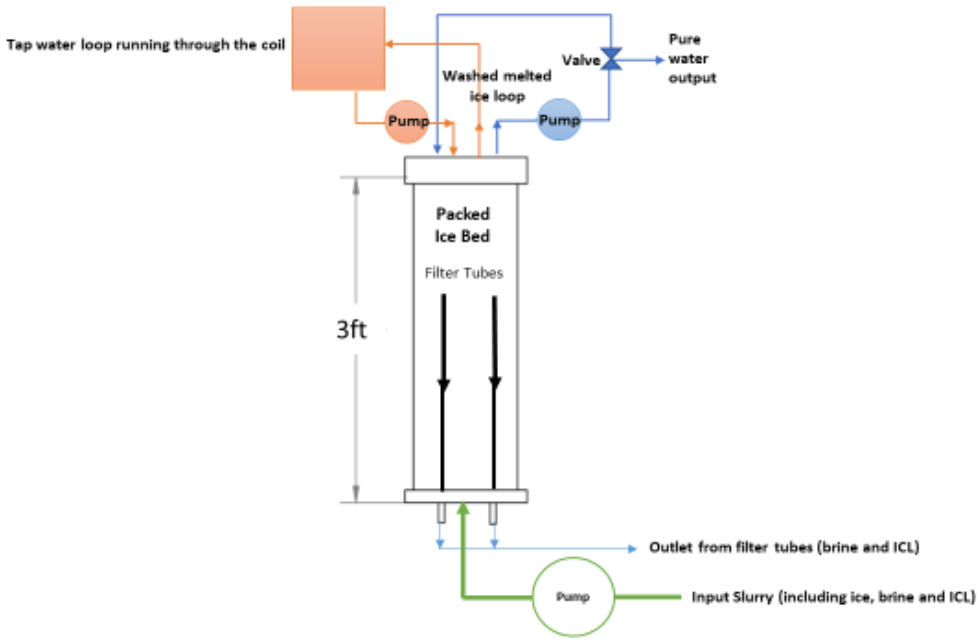

Figure 37. Schematic view of the hydraulic wash column setup

The wash column was design based on a common model called TNO-Thijssen type. This common type of hydraulic wash columns has been used in many studies before, however, the number of filter tubes are different in each study. It was decided to put 2 filter tubes considering the size of the column and also make one other important modification. The TNO-Thijssen model utilizes a scraper or moving knife at the bottom of the column to help discharging the packed bed if ice. As discussed before, there was the interest to avoid using any mechanical or moving part in our design, that was the main reason not to make a mechanical wash column although it would have saved us from using pumps. So, to achieve such desire, it was needed to find a replacement for the scraper. The hot water loop and the coil in the column was design

and manufactured to perform as an alternative to the moving part. Figure 38 shows the lab scale hydraulic wash column setup and describes the parts.

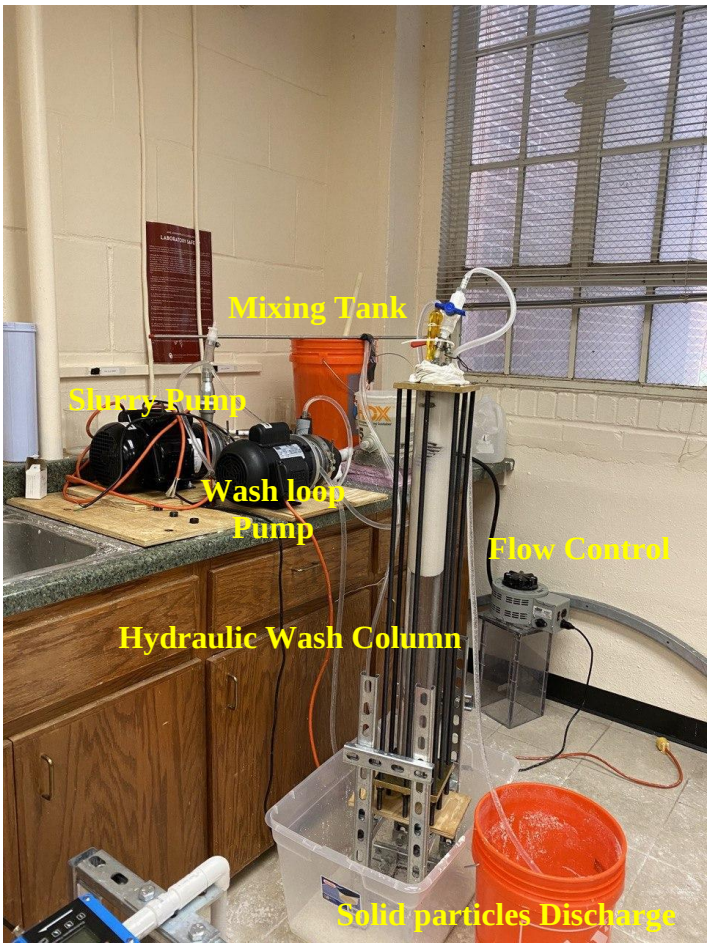

Figure 38. Hydraulic wash column setup

The wash column is 3feet long and has two 12 by 12 inches plate on top and bottom. On the top plate there are 3 plugs which one is the inlet flow, and two others are filter tube outlets. The outlets are ¾ inches each. The bottom plate has 4 plugs which the coil intel and outlet is connected to two and the other two are the inlet and outlet for pure water wash loop. The size of each inlet and outlet is ¾ inches. There were 2 pumps in the setup, which provide the flow velocities necessary for the inlet slurry and the wash loop. The pumps are 1 and 1.5 hp and are capable of handling solids up to 3/32 inches diameter. As discussed before the wash column has 2 filter tubes which help the liquid phases drain. Our filter tubes include a steel pipe and a muffler each. Mufflers have been connected to the bottom part of the pipes, Fig. 39.

Figure 39. Position of the filter tubes, coil, and outlet at the bottom section of hydraulic wash column

The mufflers were chosen to act as the filtration section in filter tubes. Each muffler has a specific separation limit. The separation limit and design of each purchased muffler is presented in Fig. 40.

(a) (b) (c)

Figure 40. Mufflers with various screen opening sizes, (a) 40-90 microns (b) 100 microns (c) 250 microns

Considering that the wash column and separation setup was tested separately and not alongside with the crystallization setup at this moment, the most important issue is to select a substitute for the ice-brine-ICL slurry. Considering the density of the ice and brine, water to act as brine and a type of PCM called palm wax was selected, Fig. 41, to act as the ice particles. The density of the wax is around 900 kg/m^3 and the density of the water is considered to be 1000 kg/m^3.

Figure 41. PCM particles act as ice particles in our wash column model.

The mixture is made in the mixture tank by adding PCM into water and also considering the densities of each phase, the mixture needs manual stirring throughout the experiments. Using the 1.5 hp pump, the slurry was running into the wash column. While the slurry starts to fill up the column the filter tubes start to discharge the liquid phase (water) into the mixing tank. Figure 42 shows the filter tube discharge product. It is shown in this picture that the separation in the column is occurring perfectly since there is no solid particles in the discharge product.

Figure 42. Filter tube discharge product

Figure 43 shows the separation of solid particles and accumulation of particles outside of the mufflers. The particles start to form the bed around the mufflers and keep building upwards towards the top plate.

Figure 43. Accumulation of solid particles around the mufflers

To control the flow, a transformer connected to the slurry pump was utilized, Fig 44a, however, as the experiments were moving forward, the need for controlling the flow more accurately led to add a VFD[11] device, Fig 44b, to control the flow rates in both pumps.

(a)

(b)

Figure 44. Flow Controlling devices (a) Transformer, (b) VFD device

Using the transformer, giving the slurry pump a 40% power load and letting the mixture run through the column, the packed bed starts to form and after a while it can be clearly observed, a sharp wash front separating the packed bed from the mother liquor, Fig. 45.

Figure 45. Formation of the packed bed of solids and wash front

[11] Variable Frequency Derive

It is worth mentioning that the filter tubes were performing well for a while but after a considerable time passed, some particles got stuck inside the filter screens and stopped the flow of the liquid phase into the filter tubes. To tackle this latter problem, the mufflers were modified with a covering fabric to avoid solid particles getting stuck in the way. Figure 46 shows the modified mufflers.

Figure 46. Mufflers with fabric covering

After the packed bed is formed and the flow reached steady state, the next step is to discharge the solid particles. To do so, a water loop (wash loop) was used in which water was running from the top inlet through the packed bed and then the solid particles are getting washed away with that water. First, this process was performed separately, meaning that the packed bed was formed and then the solid particles were discharged. The pumps were not working together at this stage. Figure 47 shows the discharged solid particles in this batchwise process.

Figure 47. Solid particles extraction using a wash loop - batchwise process

The desired next step is to continuously run the setup to form the packed bed and simultaneously discharge solid particles. This continuous setup will then join the crystallization setup and form the ZDL freeze desalination unit as described in Chapter 1. A series of experiment were conducted to run the separation setup continuously but to this time of writing the thesis the efforts are still going on. The problems occur when trying to run both pumps simultaneously, since they were initially with different powers and the slurry pump was more powerful than the wash loop pump and therefore the wash loop would get stuck and not run through the packed bed.

A solution to our problem would be to substitute the wash loop pump with a similar power to the slurry pump. Then both pumps will have same power and will not interfere with each other. One other solution is to utilize VFD devices on both pumps. At this moment the slurry pump is the only pump connected to a VFD device, connecting the wash loop pump to a similar VFD will help to give more control on the flow rates of each loop and therefore will make the process continuous.

4. Conclusions

This thesis introduced a novel ZDL method and focused specifically on separation stage of the proposed method. Two methods of separation for the solid-liquid slurries were studied and their capabilities to serve as the separation step in the freeze desalination unit were investigated. Experimental and numerical studies were performed for each separation method and results and discussions were provided. First an experimental and numerical study on hydrocyclones were performed in which a lab scale hydrocyclone setup was designed and manufactured. The numerical study was developed based on a model with the original lab scale hydrocyclone dimensions. Experimental study was performed on a small laboratory setup using a purchased hydrocyclone. The results from the experiments showed that the hydrocyclone works well when the density difference between the phases is considerable. For the case of solid particles with close density to the liquid phase, the hydrocyclone struggled to perform well. The numerical results were found to be in good agreement with the experimental results.

Since the hydrocyclone did not produce the desired separation efficiency for slurries with relatively small density difference between the solid and liquid phases, the wash column separation systems were investigated. The three main types of wash columns were introduced and the findings from previous studies were discussed. A simple numerical model was developed mainly to study the optimum inlet flow velocity in a hydraulic wash column. Separation behavior and particle bed formation and position were investigated. Results showed that for the original wash column model, a 20 m/s inlet flow velocity will form the packed bed in the lowest zone of the wash column. The effect of column base diameter (surface area) was studied. A lab scale hydraulic wash column was designed and manufactured. The setup has been built to run experiments and simulate the ice-brine-ICL slurry through the column to form a packed bed and discharge the solid particles. Batchwise separation process was successfully demonstrated.

Further work will include connecting the setup wash loop pump to a VFD and perform tests to find the optimum flow rates to control both slurry and wash loops in order to continuously run the hydraulic wash column and finalize the separation stage of the novel ZDL freeze desalination method. After that the separation and crystallization setups will be combined and tests will be performed with the actual ice-brine-ICL slurry to form the ice crystals and then separate them and extract clean water as the final product of the desalination unit.

References

[1] A. Rushton, A. S. Ward, and R. G. Holdich, *Solid-liquid filtration and separation technology*. 2008.

[2] L. yang WANG, Z. chu ZHENG, Y. xiang WU, J. GUO, J. ZHANG, and C. TANG, "Numerical and experimental study on liquid-solid flow in a hydrocyclone," *J. Hydrodyn.*, vol. 21, no. 3, pp. 408–414, 2009.

[3] G. Q. Dai, W. M. Chen, J. M. Li, and L. Y. Chu, "Experimental study of solid-liquid two-phase flow in a hydrocyclone," *Chem. Eng. J.*, vol. 74, no. 3, pp. 211–216, 1999.

[4] Q. Yang, H. L. Wang, Y. Liu, and Z. M. Li, "Solid/liquid separation performance of hydrocyclones with different cone combinations," *Sep. Purif. Technol.*, vol. 74, no. 3, pp. 271–279, 2010.

[5] T. Han, H. Liu, H. Xiao, A. Chen, and Q. Huang, "Experimental study of the effects of apex section internals and conical section length on the performance of solid–liquid hydrocyclone," *Chem. Eng. Res. Des.*, vol. 145, pp. 12–18, 2019.

[6] C. A. O. Rocha, G. Ullmann, D. O. Silva, and L. G. M. Vieira, "Effect of changes in the feed duct on hydrocyclone performance," *Powder Technol.*, vol. 374, pp. 283–289, 2020.

[7] T. C. Monredon, K. T. Hsieh, and R. K. Rajamani, "Fluid flow model of the hydrocyclone: an investigation of device dimensions," *Int. J. Miner. Process.*, vol. 35, no. 1–2, pp. 65–83, 1992.

[8] P. J. Jansens, R. Van Der Ham, O. S. L. Bruinsma, G. M. Van Rosmalen, and M. Matsuoka, "The Purification process in hydraulic packed-bed wash columns," *Chem. Eng. Sci.*, vol. 50, no. 17, pp. 2717–2729, 1995.

[9] P. J. Jansens, O. S. L. Bruinsma, and G. M. Van Rosmalen, "Compressive stresses and transport forces in hydraulic packed bed wash columns," *Chem. Eng. Sci.*, vol. 49, no. 21, pp. 3535–3543, 1994.

[10] L. Van Oord-Knol, O. S. L. Bruinsma, and P. J. Jansens, "Dynamic behavior of hydraulic wash columns," *AIChE J.*, vol. 48, no. 8, pp. 1665–1678, 2002.

[11] F. G. F. Qin, X. D. Chen, S. Premathilaka, and K. Free, "Experimental study of wash columns used for separating ice from ice-slurry," *Desalination*, vol. 218, no. 1–3, pp. 223–228, 2008.

[12] F. G. F. Qin, X. Yang, and M. Yang, "An adhesion model of the axial dispersion in wash columns of packed ice beds," *Sep. Purif. Technol.*, vol. 79, no. 3, pp. 321–328, 2011.